Gamma Knife Stereotactic radiotherapy combined with tislelizumab as later-line therapy in pMMR/MSS/MSI-L metastatic colorectal cancer: A Phase II Trial Analysis

Yiran Zhang[1,2*], Hanyang Guan[1*], Shijin Liu[1*], Haoquan Li[1], Zili Bian [1], Jiashuai He[1], Zhan Zhao[1], Shenghui Qiu[1], Tianmu Mo[1], Xiangwei Zhang[1], Zuyang Chen[1], Hui Ding[1], Xiaoxu Zhao[1], Liang Wang[3#], Yunlong Pan[1,4#], Jinghua Pan[1#]

1. Department of General Surgery, The First Affiliated Hospital of Jinan University, 510632, Guangzhou, Guangdong, P. R. China
2. Department of Body Gamma Knife, The First Affiliated Hospital of Jinan University, 510632, Guangzhou, Guangdong, P. R. China
3. Department of Oncology, The First Affiliated Hospital of Jinan University, 510632, Guangzhou, Guangdong, P. R. China
4. MOE Key Laboratory of Tumor Molecular Biology and Key Laboratory of Functional Protein Research of Guangdong Higher Education Institutes. Institute of Life and Health Engineering, Jinan University, Guangzhou, China.

*These authors contributed equally

Running title: Combined SBRT and Immunotherapy in pMMR mCRC.

[#]**Corresponding author:**
Jinghua Pan, Department of General Surgery, The First Affiliated Hospital of Jinan University, 510632, Guangzhou, Guangdong, P. R. China; E-mail: huajanve@foxmail.com
Yunlong Pan: Department of General Surgery, The First Affiliated Hospital of Jinan University, 510632, Guangzhou, Guangdong, P. R. China; E-mail: tpanyl@jnu.edu.cn
Liang Wang: Department of Oncology, The First Affiliated Hospital of Jinan University, 510632, Guangzhou, Guangdong, P. R. China. E-mail: wangliang@jnu.edu.cn.

Conflict of interest: The authors disclosed no potential conflicts of interest.

Abstract

An immunosuppressive tumor microenvironment limits the efficacy of immunotherapy, thus patients with MSS and pMMR mCRC often face great challenges.In this phase II trial, patients received Gamma Knife SBRT combined with Tislelizumab. P Biomarker analysis was performed pre- and post-treatment. From November 2022 to July 2024, 13 of 20 patients achieved PR, 6 achieved SD. mPFS was 10.7 months (95% CI, 6.4-15.0). With no grade 4 events noted, common adverse events included nausea (65%), anemia (55%), and fatigue (45%). RNA sequencing indicated enhanced immune infiltration in PR patients. For patients with pMMR/MSS/MSI-L mCRC who had not responded to first and second-line therapies, the combo of Gamma Knife SBRT and tislelizumab showed high efficacy and reasonable safety. Significant post-radiotherapy improvements in the tumor's immunosuppressive microenvironment, including lower fibrosis, normalizing of tumor vasculature, and activation of the PD-1/PD-L1 checkpoint pathway were revealed by biomarker analysis. These results imply that patients with pMMR/MSS/MSI-L mCRC who were unresponsive to the first and second-line chemotherapy, Gamma Knife SBRT with tislelizumab provides a safe and powerful later-line treatment alternative. The study is registered with ClinicalTrials.gov (identifier: ChicTR2200011777).

Keywords: Gamma Knife Stereotactic body radiation therapy; mismatch repair-proficient; tislelizumab; Metastatic colorectal cancer; Immune checkpoint inhibitors; PD-L1.

Statement of significance

This study offers a safe and powerful option for pMMR/MSS/MSI-L mCRC patients fail to first and second-line chemotherapy. And discover Gamma Knife SBRT contributed to potentially converting

the suppressive "cold" tumor immune microenvironment into an activated "hot" microenvironment conducive to immunotherapy efficacy in pMMR CRC.

Introduction

Colorectal cancer continues to represent a significant threat to life. As reported in the 2020 Global Cancer Statistics, colorectal cancer accounts for 10% of all cancer cases, ranking third in incidence, while its mortality rate is 9.4%, second only to lung cancer (1,2). Especially, 20% of newly diagnosed colorectal cancer patients present show metastases, and 40% have recurrence and metastases after local treatment (3). The FOLFOX/FOLFIRI chemotherapy regimen, which comprises oxaliplatin, 5-fluorouracil, and irinotecan is the mainstay of clinical treatment for metastatic colorectal cancer (mCRC). For patients harboring wild-type RAS and BRAF, the addition of the epidermal growth factor receptor (EGFR) inhibitor cetuximab is recommended(4,5). For patients with RAS mutations, the anti-angiogenic agent bevacizumab is advised. Nevertheless, RAS-mutant patients exhibit poorer prognoses and shorter survival times compared to their wild-type counterparts (6,7). The efficacy of chemotherapy in combination with targeted therapy remains suboptimal (7).

The development of immune checkpoint inhibitors (ICIs) transforms cancer immunotherapy (8). Particularly CRCs with mismatch repair deficiency (dMMR) and high microsatellite instability (MSI-H) show a strong response to ICIs (9). But most CRC cases are either microsatellite-stable/low microsatellite instability (MSS/MSI-L) or mismatch repair-profile (pMMR), which reduces the efficacy of immunotherapy in a significant number of mCRC patients (9). Chemotherapeutic agents can cause immunogenic cell death in tumors, thus coordinating with ICIs improves anti-tumor efficacy

(10). Additionally, anti-angiogenic therapies targeting VEGFR facilitate the normalization of tumor vasculature and promote immune cell infiltration, subsequently amplifying immune-mediated tumor eradication (11). Clinical studies, however, have revealed that t combining mFOLFOX6 or other chemotherapy regimens with anti-VEGF, anti-EGFR, and ICIs does not produce better clinical outcomes in mCRC (12,13). Consequently, identifying alternative strategies to augment the efficacy of immunotherapy remains a pivotal objective in the field of cancer immunotherapy in pMMR/MSS/MSI-L mCRC.

Stereotactic body radiation therapy (SBRT), effectively targets and eradicates tumor cells with high-dose radiation (14). Although traditional radiotherapy is sometimes linked with immunosuppressive effects (15), SBRT's exact targeting can expose tumor neoantigens, mobilize and activate immune cells, increase their infiltration into the tumor, and improve the tumor immune microenvironment (16,17). The Gamma Knife is a principal modality in SBRT, employing gamma rays generated by cobalt-60 to deliver a single, high-dose focused irradiation to the target lesion. The Gamma Knife provides several benefits over conventional radiotherapy, including hiexact stereotactic targeting, increased delivery dose to the lesion, prevention of accelerated repopulation of tumor cells, and better local control rates of tumors(18). Our team firstly observed a case with pMMR-type mCRC who exhibited local recurrence and distant metastasis following first-line and second-line chemotherapy combined with targeted therapy(19). After undergoing gamma knife SBRT followed by tislelizumab treatment, intrahepatic metastatic lesions were reduced and stabilized, the patient showed a partial response (PR) with notable reduction of recurrent lesions in the rectal wall and stabilization of intrahepatic metastases, so extending the progression-free survival (PFS)

exceeded beyond 3 months (19). These findings suggest that Gamma Knife SBRT might improve ICBs sensitivity in mCRC.

The results of a phase II clinical trial assessing the combination of Gamma Knife SBRT combined with tislelizumab as a later-line therapy in patients with pMMR/MSS/MSI-L mCRC are presented in this report together with safety and efficacy. NanoString assay for transcriptome analysis was employed to elucidate changes in the tumor immune microenvironment during the combined treatment, offering insights into the therapeutic potential and mechanistic underpinnings of this integrated approach.

Results

Patients

In this clinical trial, twenty patients with pMMR/MSS/MSI-L tumors refractory to first or second-line treatment were enrolled. The cohort comprised 15 males and 5 females, with ages ranging from 47 to 77 years. Predominantly, the primary tumors were located in the left colon and rectum (17/20, 85%), with the liver being the most common site of metastasis, followed by the lung (3/20)(**Table 1**). Flowchart of therapeutic regimen and flow diagram of enrolled participants in the study were shown in **Figure 1A** and **Figure 1B.**

Molecular profiling revealed RAS mutations in 11 patients (55%), with 5 exhibiting KRAS mutations and 6 presenting NRAS mutations. PD-L1 expression was assessed in 18 patients, 12 (60%) patients had combined positive score (CPS) ≤ 1. Tumor mutation burden (TMB) data were

available for 8 patients, with a median TMB of 4.62 mutations/Mb (IQR 3.08-8.97). Notably, only one patient exhibited a TMB > 10 mutations/Mb (**Table 1)**.

Characteristics	Patients (n=20)
Age, years, median (IQR), n (%)	60 (56-65)
<60	8 (40%)
≥60	12 (60%)
Sex, n(%)	
Male	15 (75%)
Female	5 (25%)
ECOG performance status, n (%)	
0	12 (60%)
1	8 (40%)
Primary tumor location, n (%)	
Left colon and rectum	17 (85%)
Right colon	3 (15%)
Number of metastatic organs[a], n (%)	
1	14 (70%)
≥2	6 (30%)
Metastatic organ, n (%)	
Liver	14 (70%)
Lung	7 (35%)
Lymph node	2 (10%)
Other	3 (15%)
Ras mutation type, n (%)	
KRAS	5 (25%)
NRAS	6 (30%)
Other	9 (45%)
PD-L1 expression, CPS, n (%)	
CPS≤1	12 (60%)
CPS > 1	6 (30%)
Unknown	2 (10%)
TMB (mut/Mb), median (IQR), n (%)	4.62 (3.08-8.97)
TMB<5	4 (20%)
TMB≥5, ≤10	3 (15%)
TMB>10	1 (5%)
Unknown	12 (60%)

Abbreviations: CPS, combined positive score; ECOG, Eastern Cooperative Oncology Group; IQR, interquartile range; TMB, tumor mutation burden.
[a]Multiple answers allowed.

Table 1: Baseline demographic and clinical characteristics.

Efficacy

In our cohort of 20 patients meeting inclusion criteria, 13 (65%) achieved a partial response (PR), and 6 (35%) maintained stable disease (SD), resulting in a robust disease control rate (DCR) of 95% (**Table 2**). Patients with liver metastases achieved 92.9% DCR, and patients with metastases in non-liver locations notably achieved a remarkable 100% DCR, only 1 patient with liver metastases experienced disease progression (PD) (**Figure 2A**), As of the data cutoff date, 7 patients remained on maintenance treatment, and 1 patient underwent surgery due to disease progression (**Figure 2A**). Remarkably, 3 patients refractory to first-line treatment responded to SBRT combined with tislelizumab, achieving rapid regression to NED status, with durations ranging from 6 to 18 months before progression. Encouragingly, 1 patient remains in a state of NED, under ongoing monitoring (**Figure 2A**).

	All patients (N = 20)	**Liver metastasis (N = 14)**	**Other metastasis (N = 6)**
Best overall response			
Complete response (CR), n (%)	0 (0%)	0 (0%)	0 (0%)
Partial response (PR), n (%)	13 (65%)	8 (57%)	5 (83%)
Stable disease (SD), n (%)	6 (30%)	5 (36%)	1 (17%)
Progressive disease (PD), n (%)	1 (10%)	1 (7%)	0 (0%)
ORR, n (%, 95% CI)	13 (65%, 40.8-84.6%)	8 (57.1%, 28.9-82.3%)	5(83.3%, 35.9-99.6%)

DCR, n (%, 95% CI)	19 (95%, 75.1-99.9%)	13 (92.9%, 66.1-99.8%)	6(100%, 54.1-100%)

Abbreviations: ORR, objective response rate; DCR, disease control rate.

Table 2: Efficacy outcomes.

Most patients exhibited favorable survival outcomes throughout the treatment (**Figure 2B**), and median progression-free survival (PFS) was 10.7 months (95% CI, 6.4, 15.0) (**Figure 2C**). Additionally, a comparative survival analysis included 23 patients who underwent first and second-line treatment and Gamma Knife SBRT without immunotherapy, revealing a median PFS of 6.7 months (95% CI, 5.6, 7.0), this data shown Gamma Knife SBRT combined with tislelizumab as later-line treatment prolong PFS in mCRC (Log-rank test = 5.638, P = 0.0176) (**Figure 2D**). These findings suggest Gamma Knife SBRT combined with tislelizumab can effectively inhibiting mCRC progression.

In our analysis of clinical characteristics and patient prognosis, we observed that the median progression-free survival (mPFS) of patients with wild-type RAS expression was significantly longer (14 months) compared to those with KRAS (7.3 months) and NRAS (5 months) mutations (**Figure 2-figure supplementary1 A**). These results are consistent with prior studies indicating that RAS mutations are associated with increased malignancy, diminished therapeutic response, and poorer overall prognosis in colorectal cancer. However, statistical analysis did not reveal a significant difference between the groups (Log-rank test = 4.278, P = 0.118), which may be attributed to the limited sample size and other factors inherent to the study design. Additionally, we assessed the PFS of patients with simple liver metastases versus those with metastases to other organs (**Figure 2-figure supplementary1 B**). Notably, the mPFS of patients with liver metastases (13 months) was

longer than that of those with metastases at other sites (8.5 months). This difference could potentially be explained by the efficacy of localized gamma knife treatment in managing liver metastases. Despite this observation, statistical comparison between the two groups did not yield a significant difference (Log-rank test = 0.081, P = 0.776). Given these limitations, further investigation with larger sample sizes is essential to elucidate the factors contributing to these trends and to confirm the clinical significance of these findings.

In light of the abscopal effect of radiotherapy, we extended our observations beyond the lesions directly targeted by stereotactic radiotherapy to include non-irradiated lesions (**Figure 2-figure supplementary1 C**). Imaging examinations revealed significant tumor regression in both the irradiated target lesions (**Figure 2E, F**) and the non-irradiated lesions (**Figure 2E, G**) following Gamma Knife SBRT combined with tislelizumab. These findings suggest that SBRT not only impacts the irradiated lesions but also sensitize distant metastatic sites for ICBs through the abscopal effect, thereby enhancing the systemic antitumor response when combined with immunotherapy.

Safety

All 20 enrolled patients received the assigned treatment regimen, with safety assessments conducted every three treatment cycles. Treatment-related adverse events (TRAEs) and immune-related adverse events are summarized in **Table 3.** Predominantly, patients experienced mild to moderate adverse events, with the most common being nausea (65%), anemia (55%), electrolyte disturbances (55%), fatigue (45%), and anorexia (35%). Notably, only two patients experienced grade 3 events of increased blood bilirubin, while no grade 4 adverse events were

reported throughout the study period.

TEAEs, n (%)	Patient (N=20)				
	Grade 1	Grade 2	Grade 3	Grade 4	Any grade
Anemia	9 (45%)	2 (10%)	0	0	11 (55%)
Neutropenia	1 (5%)	0	0	0	1 (5%)
Nausea	10 (50%)	3 (15%)	0	0	13 (65%)
Poor appetite	3 (15%)	4 (20%)	0	0	7 (35%)
Electrolyte disturbance	7 (35%)	2 (10%)	0	0	11 (55%)
Hand-foot syndrome	0	0	0	0	0
Leukocytopenia	2 (10%)	0	0	0	2 (10%)
Aspartate transaminase increased	2 (10%)	2 (10%)	0	0	4 (20%)
Lipase increased	0	0	0	0	0
Proteinuria	0	0	0	0	0
Thrombocytopenia	2 (10%)	2 (10%)	0	0	4 (20%)
Vomiting	1 (5%)	3 (15%)	0	0	4 (20%)
Hypothyroidism	0	0	0	0	0
Triglycerides increased	0	0	0	0	0
Fatigue	6 (30%)	3 (15%)	0	0	9 (45%)
Blood bilirubin increased	0	0	2 (10%)	0	2 (10%)
Alanine transaminase increased	2 (10%)	1 (5%)	0	0	3 (15%)
Peripheral neurotoxicity	0	0	0	0	0
Hoarseness	0	0	0	0	0
Rash	4 (20%)	0	0	0	4 (20%)
Thyroiditis	0 (0%)	0	0	0	0
Diarrhea	1 (5%)	0	0	0	1 (5%)
Troponin increased	0	0	0	0	0
Fever	0	0	0	0	0
Alkaline phosphatase increased	0	0	0	0	0
Amylase increased	0	0	0	0	0
Hypertension	0	0	0	0	0

Table 3: Treatment-emergent adverse events (TEAEs) since the initiation of protocol-specified treatment

Identification of differentially expressed genes between responder and non-response groups

To elucidate the impact of the tumor immune microenvironment on combination therapy outcomes,

we employed NanoString assay for transcriptome analysis of tumor samples obtained from 16 enrolled patients before and after treatment, totaling 32 samples (**Figure 3A**). Patients were stratified into responder (PR) and non-responder (non-PR) groups based on treatment outcomes. Gene expression differential analysis between pre- and post-treatment samples within each group identified significant alterations, detailed in the **Source data** and illustrated in **Figure 3B.**

Our findings highlighted notable up-regulation of key genes involved in antigen presentation (CD40, TNFSF18, TNFSF4), immune checkpoint modulation (PDCD1LG2, CD274, IDO1, VTCN1), and T cell activation pathways (TNFRSF9, CD28, ICOS, CD40LG, CD2, GZMK, ENTPD1, ITGAE) in the responder group. Additionally, a diverse array of chemokine family genes (IL2, IL4, IL17A, CCR2, CCL22) showed enhanced expression in PR group (**Figure 3B**). Furthermore, immune cell abundance analysis based on 11 predefined immune cell types revealed significantly elevated levels in the PR group compared to non-PR. included T cells, B cells, mast cells, macrophages, Dendritic Cell (DC), Cytotoxic cells, NK CD56 cell, CD8 T cell, CD45 cell, Th1 cells and NK cell (**Figure 3C**). This heightened immune activation in responders encompassed robust antigen presentation, T cell activation, and co-stimulation processes crucial for effective immune-mediated tumor control.

To investigate the impact of Gamma Knife treatment on patient outcomes, we conducted a differential expression analysis of pre- and post-treatment samples from both responder (PR) and non-responder (non-PR) groups (**Figure 3-figure supplementary1 A**). The results revealed limited gene expression alterations following treatment. However, intersecting the differentially expressed genes from both groups identified NOS2 as a gene that was consistently upregulated post-treatment

in both cohorts (**Figure 3-figure supplementary1 B**). Although NOS2's increased expression may be associated with Gamma Knife treatment, its potential role in colorectal cancer treatment remains underexplored, warranting further investigation to elucidate the underlying mechanisms.

Additionally, to identify genes linked to treatment efficacy, we performed univariate and multivariate Cox regression analyses on the expression levels of 289 genes from sequencing data in relation to disease progression. Unfortunately, due to the limited sample size and sequencing depth, neither analysis yielded statistically significant results. The full Cox regression analysis of these genes is provided in the **Supplementary File1**.

Following the combination of stereotactic radiotherapy and immunotherapy, a striking reduction in liver metastasis target lesions was observed in two patients compared to baseline. To elucidate these findings, we conducted CD8 and PD-L1 immunohistochemical staining on liver metastasis biopsy specimens from some patients pre- and post-treatment (**Fig 3D-E**). The analysis revealed increased infiltration of T cells and improved immune microenvironment following treatment, aligning with our prior analytical findings.

Additional immune signatures analysis in predicting tumor response

We conducted gene expression analysis based on 12 predefined gene sets associated with immunotherapy and prognosis (**Figure 4A**). Notably, samples from the responder group exhibited higher expression of immune activation related genes compared to the non-responder group, include effector T cells (T-eff), T cell-Inflamed, IFN-γ，cytotoxic, Cytolytic activity score (CYT), chemokines,

angiogenesis (AG), APC co-stimulation (APC co-sti), inflammation promoting (Inflam-pro), T cell co-stimulation (T cell co-sti), parainflammation (parainflam) and tumor-infiltrating lymphocytes (TIL) (**Figure 4A**).

Further compared the related-signature score, we found the responders had higher APC and T cell co-stimulation signature scores compared with the non-responder group **(Figure 4B**). Moreover, the responders had higher T cell-Inflamed, inflammation promoting and parainflammation signature scores compared with the non-responder group (**Figure 4C**). Additionally, increased expression of effector T cell, cytotoxicity, IFN-γ production, and cytolytic activity and TIL signature scores compared with the non-responder group (**Figure 4D**).

Further functional insights into differential gene expression between responder and non-responder groups were gained through gene ontology (GO) enrichment and Kyoto Encyclopedia of Genes and Genomes (KEGG) pathway analyses. GO analysis highlighted enrichment in cytokine and chemokine receptor activities, alongside increased T cell and leukocyte proliferation and activation levels in responders (**Figure 4-figure supplementary1 A**). Correspondingly, KEGG analysis underscored enrichment in pathways involving antigen processing and presentation, T cell receptor signaling, chemokine interactions, and cytokine signaling (**Figure 4-figure supplementary1 B**). Notably, these results indicated responders after combination of Gamma Knife SBRT and tislelizumab treatment will enhancing tumor antigen presentation and T cell mediated immune response in pMMR/MSS/MSI-L mCRC.

Analysis on differential expression genes before and after treatment in the responders.

To unravel the mechanisms driving tumor regression in the responder cohort, we conducted comprehensive gene expression analysis before and after treatment, focusing on 7 gene groups known for their potential inhibitory effects on immunotherapy. Post-treatment analysis revealed significant reductions in exhausted T cells, Th2 cells, and Treg cells, indicative of a favorable shift away from a suppressive immune microenvironment (**Figure 5A**). Tumor resistance mechanisms, such as fibrosis and angiogenesis, play pivotal roles in limiting therapeutic efficacy(20,21). Initially, evaluation of immunotherapy-related gene groups in partial responders versus non-responders highlighted significantly higher angiogenesis scores in the former, albeit with no significantly difference (**Figure 5B**). Recognizing potential biases from pooling samples pre- and post-treatment, we conducted separate analyses within the responder group, expanding our gene set to include fibrosis-related genes. The findings underscored substantial inhibition of both angiogenesis and fibrosis within the tumor microenvironment following SBRT, targeted therapy, and immunotherapy (**Figure 5C**). We also analyzed tumor samples from select patients before and after treatment, employing immunohistochemical staining for CD31, a marker of vascular survival (**Figure 5D**). The results demonstrated a significant reduction in CD31 expression following Gamma Knife irradiation, further supporting the notion that Gamma Knife treatment, when combined with immunotherapy, can effectively inhibit tumor angiogenesis (**Figure 5E**).

Further stratified analysis of non-responder samples before and after treatment revealed no significant alterations in the expression levels of immunosuppression-related or angiogenesis/fibrosis-related gene sets (**Figure 5-figure supplementary**1). These insights

illuminate critical pathways through which combined therapies modulate the immune landscape and enhance treatment responses in pMMR/MSS/MSI-L mCRC.

Discussion:

By successfully reaching its main endpoint, this phase II trial shows that for combined Gamma Knife SBRT with tislelizumab greatly increases progression-free survival (PFS) in pMMR/MSS/MSI-L mCRC, resistant to first and second-line therapies. For this patient population, the combo treatment has shown both safety and tolerability. By overcoming resistance to first treatment plans, our study presents a creative therapy approach for those unresponsive to conventional treatments that offers a suitable therapeutic option improving clinical outcomes.

Among the several cancers including nasopharyngeal carcinoma, esophageal cancer, liver cancer, and lung cancer, Tislelizumab, a new PD-1 inhibitor, has been shown especially therapeutic efficacy. Combining tislelizumab with chemotherapy has essentially extended PFS in patients across these cancers (22-25).While immunotherapy has proven beneficial for some patients, metastatic colorectal cancer (mCRC) presents unique challenges. Particularly in patients with MSS/pMMR tumors, which are marked by low immunogenicity and great resistance to immunotherapy, tumor cells in mCRC often evade immune detection and destruction (26). By directly targeting and destroying tumor cells, Gamma Knife SBRT presents a potential solution by releasing a significant volume of tumor neoantigens, and improving tumor immunogenicity, so optimizing maximizing the efficacy of subsequent immunotherapy(27). Furthermore demonstrated to extend survival in non-small cell lung cancer (NSCLC) with patients with brain metastases is the combination of Gamma Knife SBRT and

immunotherapy (28). Still underreported, though, is the possibility of Gamma Knife SBRT coupled with ICIs to improve the response in pMMR/MSS/MSI-L CRC.

In our clinical observations, a notable therapeutic effect was achieved in a patient treated with combined SBRT and immunotherapy. We hypothesize that the addition of tislelizumab following SBRT could extend progression-free survival (PFS) compared to either modality alone. Tumor microenvironment post-radiotherapy showed significant changes revealed by sequencing analysis of tumor samples ‘both before and after combined treatment. More precisely, the microenvironment transitioned from an immunosuppressive, angiogenesis- and fibrosis-promoting state to an immune-enhanced, angiogenesis- and fibrosis-attenuated state. Comparatively to non-responders, responders expressed genes linked to antigen presentation, tumor inflammation, and immune-mediated tumor killing more strongly. Further showing the activation of several signaling pathways associated with tumor cell death, including NF-κB, TNF, and JAK-STAT pathways was enrichment analysis. Furthermore, immunotherapy targets such as PD-L1, showed an elevation, which supports the possibility of efficient later immunotherapy. These findings substantiate our hypothesis that patients with MSS-type mCRC resistant to first-line treatment could benefit significantly from the combination of stereotactic radiotherapy and immunotherapy, with enhanced immunogenicity and a more favorable tumor microenvironment facilitating improved therapeutic outcomes.

This trial restrictions even if its outcomes show promise. First of all, our results could be biased as a single-arm study devoid of a control group. Second, the limited sample size and single-center design

of the study lower its statistical power hence more robust conclusions depend on bigger studies. Furthermore, even though general survival (OS) was examined, the follow-up duration was insufficient to establish a reliable median OS. Subgroup analysis stratified by mutation type and metastatic site did not yield statistically significant prognostic results, likely due to limitations in both the available patient data and the sequencing depth. Given the importance of identifying reliable biomarkers for predicting the efficacy of Gamma Knife treatment, we attempted to address this gap by establishing a Cox proportional hazards regression model. This model aimed to correlate specific genetic and clinical features with treatment outcomes. Despite these efforts, no substantial or statistically significant findings emerged from the analysis, indicating that additional data and more comprehensive modeling may be required to uncover potential predictors of treatment response. To address these limitations, a multi-center, randomized controlled trial with a larger cohort and extended follow-up period is essential. This will provide a more comprehensive evaluation of the efficacy and safety of combining Gamma Knife SBRT and tislelizumab as a later-line therapy in pMMR/MSS/MSI-L mCRC patients.

Ultimately, for patients with pMMR/MSS/MSI-L mCRC who were unresponsive to first-line therapy regimens, the combination of Gamma Knife SBRT with tislelizumab demonstrated a high disease control rate (DCR) and manageable safety profile. Significant post-radiotherapy improvements in the tumor's suppressive immune microenvironment, reduced fibrosis, normalized tumor vasculature, and activation of the PD-1/PD-L1 checkpoint pathway revealed by biomarker analyses so improving the efficacy of immunotherapy.

Methods

Study design and participants

This single-arm, phase II trial was conducted at the First Affiliated Hospital of Jinan University to assess the antitumor efficacy and safety of a combined regimen consisting of SBRT and tislelizumab in patients with pMMR/MSS/MSI-L-type metastatic colorectal cancer (mCRC). The study is registered with ClinicalTrials.gov (identifier: ChicTR2200011777). Eligible patients, aged 18-75 years, had confirmed metastatic colorectal cancer. MSS and RAS mutation statuses were determined through gene sequencing, while clinical staging was based on imaging examinations and intraoperative findings. A total of 20 patients were enrolled in the study, with all providing written informed consent. Detailed inclusion and exclusion criteria are available in the **Appendix**.

Procedures：

As illustrated in **Figure 1A**, eligible patients received SBRT (administered 5-6 times per week, 3-5 Gy per session) combined with tislelizumab (200 mg on day 1) was incorporated into the treatment regimen. Each three-week cycle comprised a maximum of 12 cycles of induction therapy. Patients achieving complete response (CR), partial response (PR), or stable disease (SD) transitioned to tislelizumab maintenance therapy (200 mg on day 1) until documented disease progression, death, unacceptable toxicity, or patient withdrawal of consent. Treatment response was evaluated using CT or MRI after each treatment cycle. Adverse events were systematically monitored and graded according to the National Cancer Institute Common Terminology Criteria for Adverse Events (version 5.0).

The study enrolled 20 eligible patients on November 24, 2022 (Figure 1B). All patients received at least one dose of the prescribed regimen. As of the data cutoff date (July 24, 2024), six patients continued to receive maintenance therapy. The median follow-up duration was 15 months (range: 3.4-20.0 months, IQR: 9.6-18.2 months). Due to disease-related complications, specimens could not be obtained from four patients, resulting in 16 patients being included in the per-protocol set (PPS).

Outcomes：

The primary endpoints of the study were objective response rate (ORR) and safety, encompassing adverse events and serious adverse events, assessed according to RECIST version 1.1. Secondary endpoints included disease control rate (DCR) and progression-free survival (PFS). ORR was defined as the proportion of patients who achieved a best objective response of complete response (CR) or partial response (PR) per RECIST criteria (version 1.1). DCR was defined as the proportion of patients who achieved CR, PR, or stable disease (SD) according to RECIST criteria (version 1.1). PFS was defined as the time from enrollment to the first documented disease progression per RECIST version 1.1 or to death from any cause, whichever occurred first.

CD8, PD-L1 & CD31 expression level：

Tumoral CD8 & CD31 expression was measured by immunohistochemistry (IHC) (22C3 pharmDx assays). The sections were scored for staining intensity according to the following scale: 0 (no staining), 1 (weak staining, light yellow), 2 (moderate staining, yellowish brown), and 3 (strong staining, brown), with 0 and 1 considered low expression, and 2 and 3 considered high expression. The score is divided into 4 levels according to the percentage of positive cells: 0%≤positive cell percentage≤25%, 1 point; 25%<positive cell percentage≤50%, 2 points; 50%<positive cell percentage≤75%, 3 points; 75%<positive cell percentage≤100%, 4 points. IHC score = cell staining intensity score x positive cell percentage score. The PD-L1 combined positive score (CPS) was defined as the number of PD-L1 positive cells (tumor cells, lymphocytes, macrophages) as a proportion of the total number of tumor cells multiplied by 100. Positive PD-L1 expression was considered when the CPS was >1.

Nanostring panel RNA sequencing：

Due to disease-related limitations, specimens could not be obtained from four patients, resulting in a cohort of 16 patients for combined analysis. Tumor tissue samples were collected both before treatment (BT) and after treatment (AT). Gene expression of each sample was measured using the

NanoString nCounter platform (NanoString Technologies, Seattle, WA). The quantitative transcriptome data were obtained based on the 289-immuno-gene panel, which includes 289 genes related to the tumor, tumor microenvironment, and immune responses in cancer. The samples that passed the quality control (QC), which included Imaging QC, Binding Density QC, Positive Control Linearity QC, and Positive Normalization QC can be processed in further analysis. Statistical analyses were conducted using R (version 3.6.1). The raw count data of 289 genes were normalized using the R package NanoStringNorm according to the geometric mean of five housekeeping genes. The log2 transformation was then performed on the normalized data. Differentially expressed genes were identified using the "DEseq2" package, employing criteria of log2|fold change| > 1 and false discovery rate < 0.05. Heatmaps depicting the expression patterns of these differentially expressed genes were generated using the "ComplexHeatmap" package.

Cox Proportional Hazards Model

Statistical analyses were conducted using R (version 3.6.1). The R package “survival” was used to generate univariate and multivariate COX analysis results, and the relevant data were saved in the **Supplementary File1**.

Immune cell profile analyses and Additional immune signatures analysis

The determination of immune cell types and gene sets associated with immunotherapy response was informed by established literature sources (29,30). We transformed each attribute (immune signature or gene set) value (GSVA score) xi into xi′ by the equation xi′ □=□(xi□−□xmin)/(xmax□−□xmin), where xmin and xmax represent the minimum and maximum of the ssGSEA scores for the gene set across all samples, respectively. The detailed gene signature list can be found in the **Supplementary File2**.

Gene set enrichment and pathway analysis

The Kyoto Encyclopedia of Genes and Genomes (KEGG) / Gene Ontology (GO) enrichment analysis was performed using the Clusterprofiler R package. The list of gene IDs was used as the input file. The Benjamini-Hochberg method was employed to adjust the p-values. The cut-off threshold of p-values was set to 0.05. The enrichment results were visualized by the ggplot2 R package. The enrichment statistic was set to classic.

Statistical analyses

Progression-free survival (PFS) and OS was estimated utilizing the Kaplan-Meier method. Statistical analyses were conducted using R (version 3.6.1). Differences between subgroups in terms of efficacy response were assessed using the nonparametric Wilcoxon rank-sum test (Mann-Whitney U test), while comparisons between pre- and post-treatment samples were analyzed with the Wilcoxon signed-rank test. Confidence intervals (CIs) for response rates were calculated employing the Clopper-Pearson method, with all reported P values being two-sided. A P value < 0.05 was considered statistically significant.

Data availability

The data generated in this study are available within the article and its **Source data**. Additional data or resources related to this article are available upon reasonable request from the corresponding authors.

Acknowledgments

This research was supported by the Clinical Frontier Technology Program of the First Affiliated Hospital of Jinan University (No. JNU1AF-CFTP-2022-a01223), the National Natural Science Foundation of China (82204436), Natural Science Foundation of Guangdong Province (2024A1515030010, 2022A1515011695), Science and Technology Projects in Guangzhou (2024A03J0825).

Ethics approval and consent to participate

This trail was conducted in accordance with the Declaration of Helsinki after approval by the Institutional Review Board of The First Affiliated Hospital of Jinan University (KY-2022-236). All patients provided written informed consent. The ClinicalTrials.gov identifier was: ChiCTR2200066117.

References

1. Sung H, Ferlay J, Siegel RL, Laversanne M, Soerjomataram I, Jemal A, *et al.* Global Cancer Statistics 2020: GLOBOCAN Estimates of Incidence and Mortality Worldwide for 36 Cancers in 185 Countries. CA: a cancer journal for clinicians **2021**;71(3):209-49 doi 10.3322/caac.21660.
2. Siegel RL, Miller KD, Goding Sauer A, Fedewa SA, Butterly LF, Anderson JC, *et al.* Colorectal cancer statistics, 2020. CA: a cancer journal for clinicians **2020**;70(3):145-64 doi 10.3322/caac.21601.
3. Biller LH, Schrag D. Diagnosis and Treatment of Metastatic Colorectal Cancer: A Review. Jama **2021**;325(7):669-85 doi 10.1001/jama.2021.0106.
4. Diagnosis, Treatment Guidelines For Colorectal Cancer Working Group C. Chinese Society of Clinical Oncology (CSCO) diagnosis and treatment guidelines for colorectal cancer 2018 (English version). Chinese journal of cancer research = Chung-kuo yen cheng yen chiu **2019**;31(1):117-34 doi 10.21147/j.issn.1000-9604.2019.01.07.
5. Benson AB, Venook AP, Al-Hawary MM, Arain MA, Chen YJ, Ciombor KK, *et al.* Colon Cancer, Version 2.2021, NCCN Clinical Practice Guidelines in Oncology. Journal of the National Comprehensive Cancer Network : JNCCN **2021**;19(3):329-59 doi 10.6004/jnccn.2021.0012.
6. Cox AD, Fesik SW, Kimmelman AC, Luo J, Der CJ. Drugging the undruggable RAS: Mission possible? Nature reviews Drug discovery **2014**;13(11):828-51 doi 10.1038/nrd4389.
7. Modest DP, Ricard I, Heinemann V, Hegewisch-Becker S, Schmiegel W, Porschen R, *et al.* Outcome according to KRAS-, NRAS- and BRAF-mutation as well as KRAS mutation variants: pooled analysis of five randomized trials in metastatic colorectal cancer by the AIO colorectal cancer study group. Annals of oncology : official journal of the European Society for Medical Oncology **2016**;27(9):1746-53 doi 10.1093/annonc/mdw261.
8. Asaoka Y, Ijichi H, Koike K. PD-1 Blockade in Tumors with Mismatch-Repair Deficiency. The New England journal of medicine **2015**;373(20):1979 doi 10.1056/NEJMc1510353.
9. Ganesh K, Stadler ZK, Cercek A, Mendelsohn RB, Shia J, Segal NH, *et al.* Immunotherapy in colorectal cancer: rationale, challenges and potential. Nature reviews Gastroenterology & hepatology **2019**;16(6):361-75 doi 10.1038/s41575-019-0126-x.
10. Yi M, Zheng X, Niu M, Zhu S, Ge H, Wu K. Combination strategies with PD-1/PD-L1 blockade: current advances and future directions. Molecular cancer **2022**;21(1):28 doi 10.1186/s12943-021-01489-2.
11. Limagne E, Euvrard R, Thibaudin M, Rébé C, Derangère V, Chevriaux A, *et al.* Accumulation of MDSC and Th17 Cells in Patients with Metastatic Colorectal Cancer Predicts the Efficacy of a FOLFOX-Bevacizumab Drug Treatment Regimen. Cancer research **2016**;76(18):5241-52 doi 10.1158/0008-5472.Can-15-3164.
12. Hamid MA, Pammer LM, Lentner TK, Doleschal B, Gruber R, Kocher F, *et al.* Immunotherapy for Microsatellite-Stable Metastatic Colorectal Cancer: Can we close the Gap between Potential and Practice? Current oncology reports **2024** doi 10.1007/s11912-024-01583-w.
13. Antoniotti C, Rossini D, Pietrantonio F, Catteau A, Salvatore L, Lonardi S, *et al.* Upfront FOLFOXIRI plus bevacizumab with or without atezolizumab in the treatment of patients with metastatic colorectal cancer (AtezoTRIBE): a multicentre, open-label, randomised, controlled, phase 2 trial. The Lancet Oncology **2022**;23(7):876-87 doi 10.1016/s1470-2045(22)00274-1.
14. Papiez L, Timmerman R, DesRosiers C, Randall M. Extracranial stereotactic radioablation: physical principles. Acta oncologica (Stockholm, Sweden) **2003**;42(8):882-94 doi 10.1080/02841860310013490.
15. Mac Manus M, Lamborn K, Khan W, Varghese A, Graef L, Knox S. Radiotherapy-associated neutropenia and thrombocytopenia: analysis of risk factors and development of a predictive model. Blood **1997**;89(7):2303-10.
16. Singh AK, Winslow TB, Kermany MH, Goritz V, Heit L, Miller A, *et al.* A Pilot Study of Stereotactic Body Radiation Therapy Combined with Cytoreductive Nephrectomy for Metastatic Renal Cell Carcinoma. Clinical cancer research : an official journal of the American Association for Cancer Research **2017**;23(17):5055-65 doi

503 10.1158/1078-0432.Ccr-16-2946.
504 17. Choi CW, Jeong MH, Park YS, Son CH, Lee HR, Koh EK. Combination Treatment of Stereotactic Body Radiation
505 Therapy and Immature Dendritic Cell Vaccination for Augmentation of Local and Systemic Effects. Cancer
506 research and treatment **2019**;51(2):464-73 doi 10.4143/crt.2018.186.
507 18. Morinaga N, Tanaka N, Shitara Y, Ishizaki M, Yoshida T, Kouga H*, et al.* Ten-Year Survival of a Patient Treated with
508 Stereotactic Gamma Knife Radiosurgery for Brain Metastases from Colon Cancer with Ovarian and Lymph Node
509 Metastases: A Case Report. Case reports in gastroenterology **2016**;10(1):199-206 doi 10.1159/000445976.
510 19. Liu S, Zhang Y, Lin Y, Wang P, Pan Y. Case report: The MSI-L/p-MMR metastatic rectal cancer patient who failed
511 systemic therapy responds to anti-PD-1 immunotherapy after stereotactic body radiation-therapy. Frontiers in
512 immunology **2022**;13:981527 doi 10.3389/fimmu.2022.981527.
513 20. Herzog BH, Baer JM, Borcherding N, Kingston NL, Belle JI, Knolhoff BL*, et al.* Tumor-associated fibrosis impairs
514 immune surveillance and response to immune checkpoint blockade in non-small cell lung cancer. Science
515 translational medicine **2023**;15(699):eadh8005 doi 10.1126/scitranslmed.adh8005.
516 21. Kopecka J, Salaroglio IC, Perez-Ruiz E, Sarmento-Ribeiro AB, Saponara S, De Las Rivas J*, et al.* Hypoxia as a driver
517 of resistance to immunotherapy. Drug resistance updates : reviews and commentaries in antimicrobial and
518 anticancer chemotherapy **2021**;59:100787 doi 10.1016/j.drup.2021.100787.
519 22. Yang Y, Pan J, Wang H, Zhao Y, Qu S, Chen N*, et al.* Tislelizumab plus chemotherapy as first-line treatment for
520 recurrent or metastatic nasopharyngeal cancer: A multicenter phase 3 trial (RATIONALE-309). Cancer cell
521 **2023**;41(6):1061-72.e4 doi 10.1016/j.ccell.2023.04.014.
522 23. Wang J, Lu S, Yu X, Hu Y, Sun Y, Wang Z*, et al.* Tislelizumab Plus Chemotherapy vs Chemotherapy Alone as
523 First-line Treatment for Advanced Squamous Non-Small-Cell Lung Cancer: A Phase 3 Randomized Clinical Trial.
524 JAMA oncology **2021**;7(5):709-17 doi 10.1001/jamaoncol.2021.0366.
525 24. Shen L, Kato K, Kim SB, Ajani JA, Zhao K, He Z*, et al.* Tislelizumab Versus Chemotherapy as Second-Line
526 Treatment for Advanced or Metastatic Esophageal Squamous Cell Carcinoma (RATIONALE-302): A Randomized
527 Phase III Study. Journal of clinical oncology : official journal of the American Society of Clinical Oncology
528 **2022**;40(26):3065-76 doi 10.1200/jco.21.01926.
529 25. Qin S, Kudo M, Meyer T, Bai Y, Guo Y, Meng Z*, et al.* Tislelizumab vs Sorafenib as First-Line Treatment for
530 Unresectable Hepatocellular Carcinoma: A Phase 3 Randomized Clinical Trial. JAMA oncology
531 **2023**;9(12):1651-9 doi 10.1001/jamaoncol.2023.4003.
532 26. Zhao W, Jin L, Chen P, Li D, Gao W, Dong G. Colorectal cancer immunotherapy-Recent progress and future
533 directions. Cancer letters **2022**;545:215816 doi 10.1016/j.canlet.2022.215816.
534 27. Kievit H, Muntinghe-Wagenaar MB, Hijmering-Kappelle LBM, Hiddinga BI, Ubbels JF, Wijsman R*, et al.* Safety
535 and tolerability of stereotactic radiotherapy combined with durvalumab with or without tremelimumab in
536 advanced non-small cell lung cancer, the phase I SICI trial. Lung cancer (Amsterdam, Netherlands)
537 **2023**;178:96-102 doi 10.1016/j.lungcan.2023.02.004.
538 28. Cho A, Untersteiner H, Hirschmann D, Shaltout A, Göbl P, Dorfer C*, et al.* Gamma Knife Radiosurgery for Brain
539 Metastases in Non-Small Cell Lung Cancer Patients Treated with Immunotherapy or Targeted Therapy. Cancers
540 **2020**;12(12) doi 10.3390/cancers12123668.
541 29. He Y, Jiang Z, Chen C, Wang X. Classification of triple-negative breast cancers based on Immunogenomic
542 profiling. Journal of experimental & clinical cancer research : CR **2018**;37(1):327 doi
543 10.1186/s13046-018-1002-1.
544 30. Zeng TM, Yang G, Lou C, Wei W, Tao CJ, Chen XY*, et al.* Clinical and biomarker analyses of sintilimab plus
545 gemcitabine and cisplatin as first-line treatment for patients with advanced biliary tract cancer. Nature
546 communications **2023**;14(1):1340 doi 10.1038/s41467-023-37030-w.

Figure legends

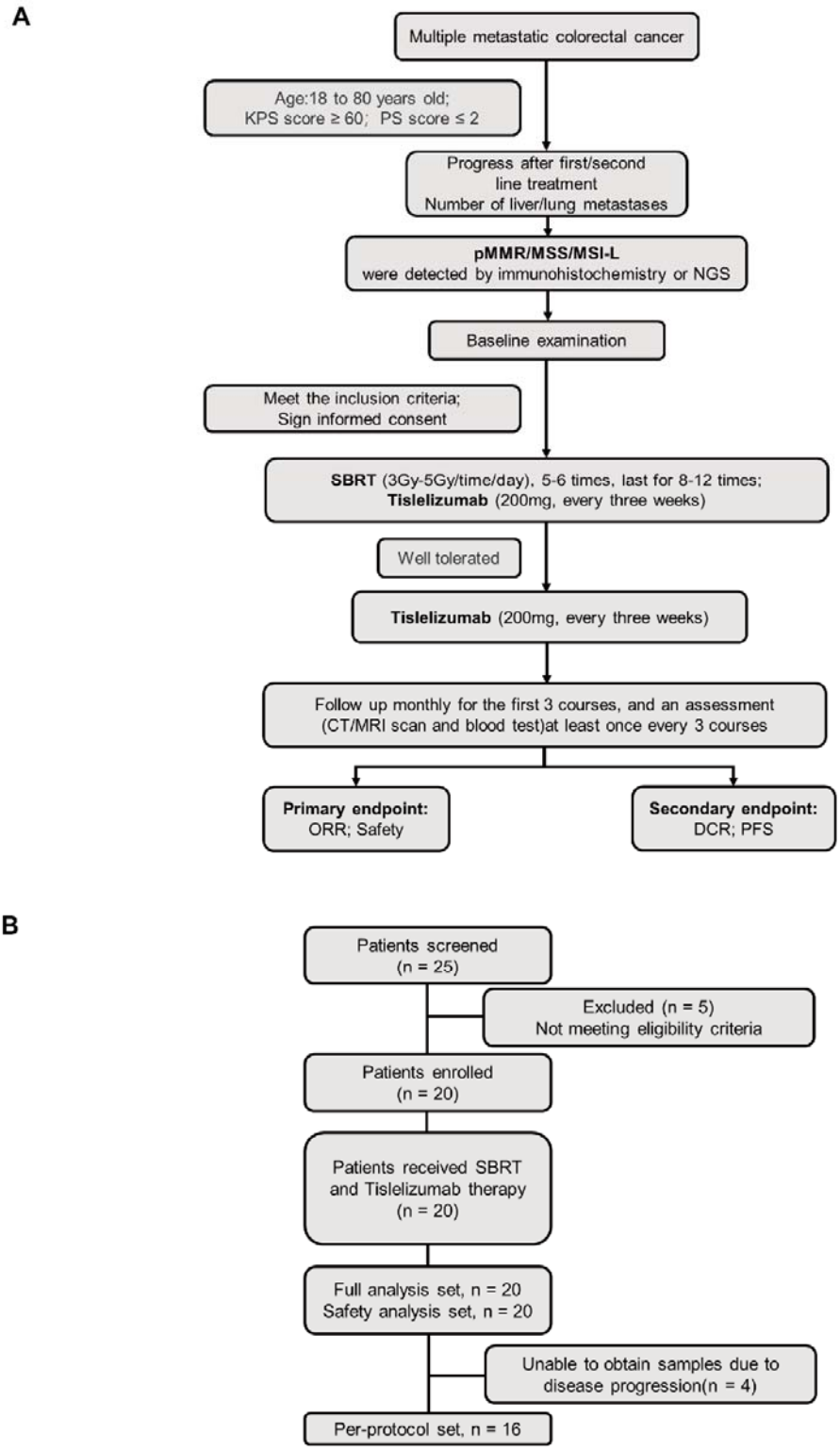

Figure 1. Clinical trial flow chart. A) Flowchart of therapeutic regimen. **B)** Flow diagram of participants in the study.

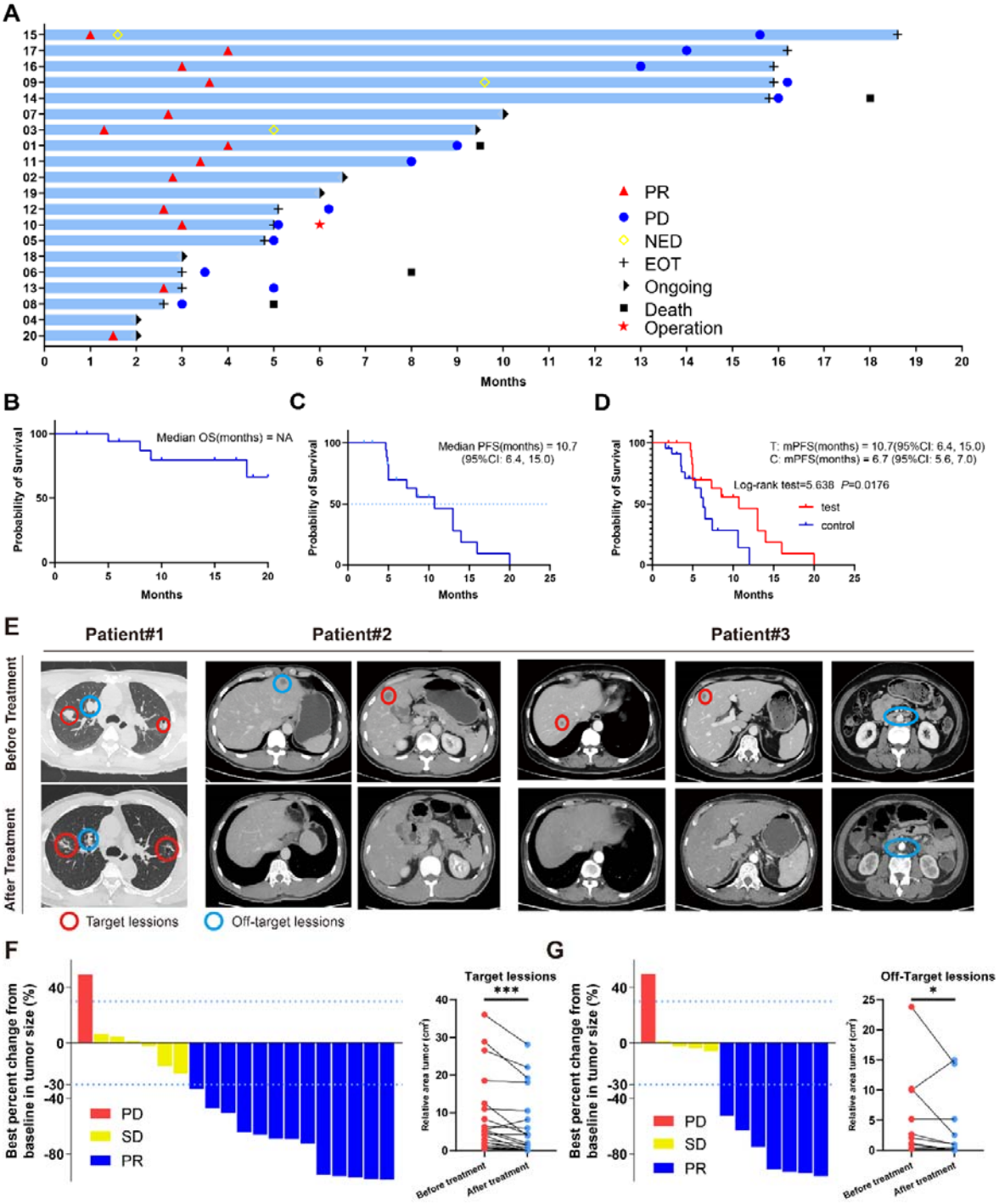

Figure 2. Clinical trial results. A) Swimmer plots of patients. **B)** Kaplan–Meier curves of OS for the per-protocol set (N = 20). **C)** Kaplan–Meier curves of PFS for the per-protocol set (N = 20). **D)** Kaplan–Meier curves of PFS for didn't receive immunotherapy set (control group) (N= 23) and per-protocol set (test group) (N=20). **E)** Radiological response from patient. **F)** Waterfall plot of best percent change from baseline in patient target lesion (N= 20). **G)** Waterfall plot of best percent change from baseline in patient off-target lesion (N= 12).

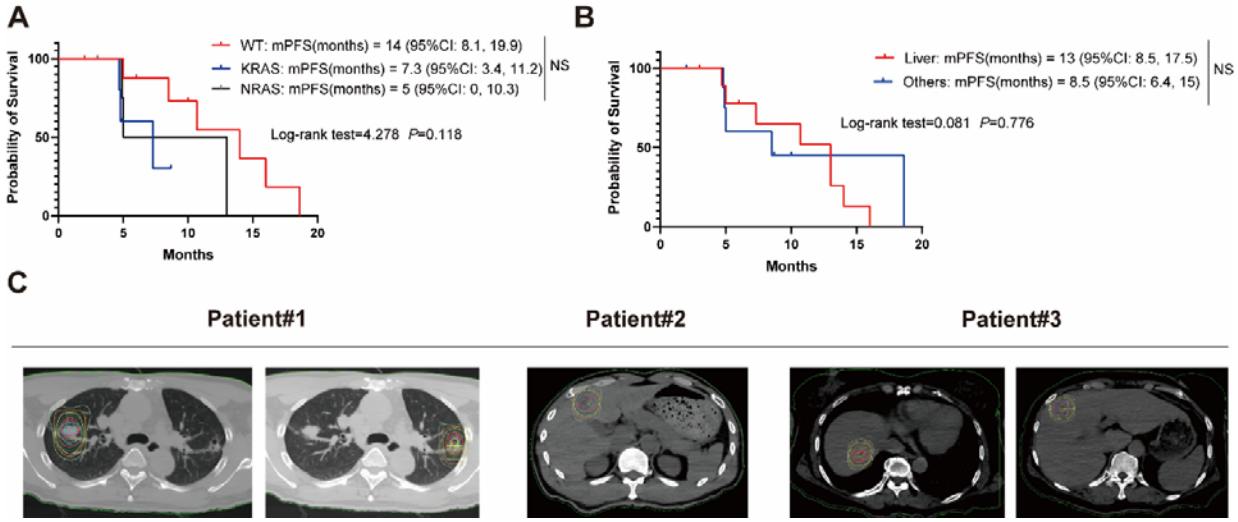

Figure 2-figure supplementary1. Supplementary Clinical trial results. **A)** Kaplan–Meier curves of PFS for RAS wite-type set (n= 9), KRAS set (n= 5) and NRAS set (n=6). **B)** Kaplan–Meier curves of PFS for simple Liver metastasis (n= 10) and othe metastasis (n= 10). **C)** Schematic diagram of isodose lines of the planned treatment volume (PTV).

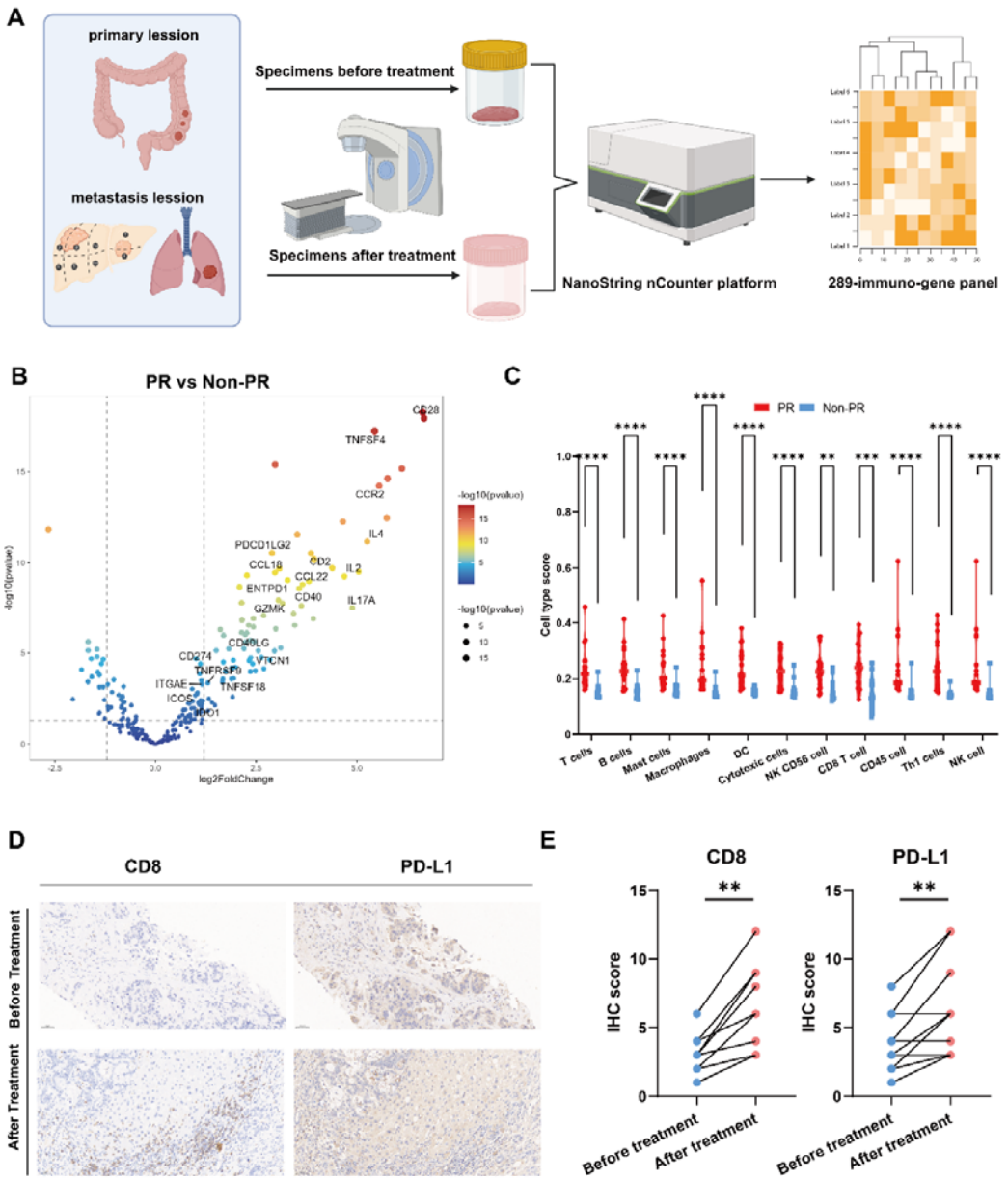

Figure 3. Differential expressed genes analysis. A) Specimens collection flowchart. **B)** Transcriptome analysis on differential expression genes between responders (PR) (n = 9) and non-responders (Non-PR) (n = 7), DESeq2 was provided to perform differential expression testing. **C)** The abundance of predefined 12 immune cells composition before and after treatment between responders (PR) (n = 9) and non-responders (Non-PR) (n = 7), Wilcoxon test was used to determine the statistical significance between subgroups. **D&E)** Representative CD8 & PD-L1 IHC staining of before and after treatment specimens of patient**.**

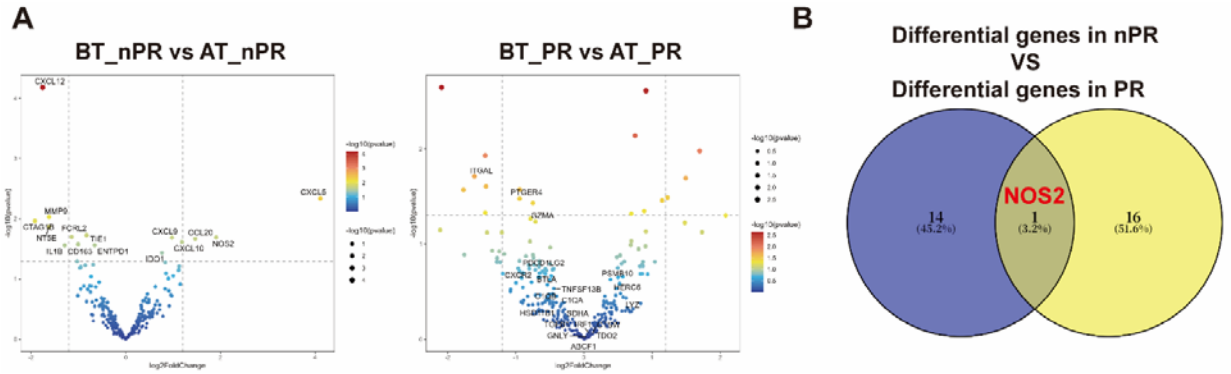

Figure 3-figure supplementary1. Supplementary Differential expressed genes analysis. A) Transcriptome analysis on differential expression genes before and after treatment between non-responders (Non-PR) (n = 7 and responders (PR) (n = 9), DESeq2 was provided to perform differential expression testing. **B)** Venn diagram of two groups of differentially expressed genes.

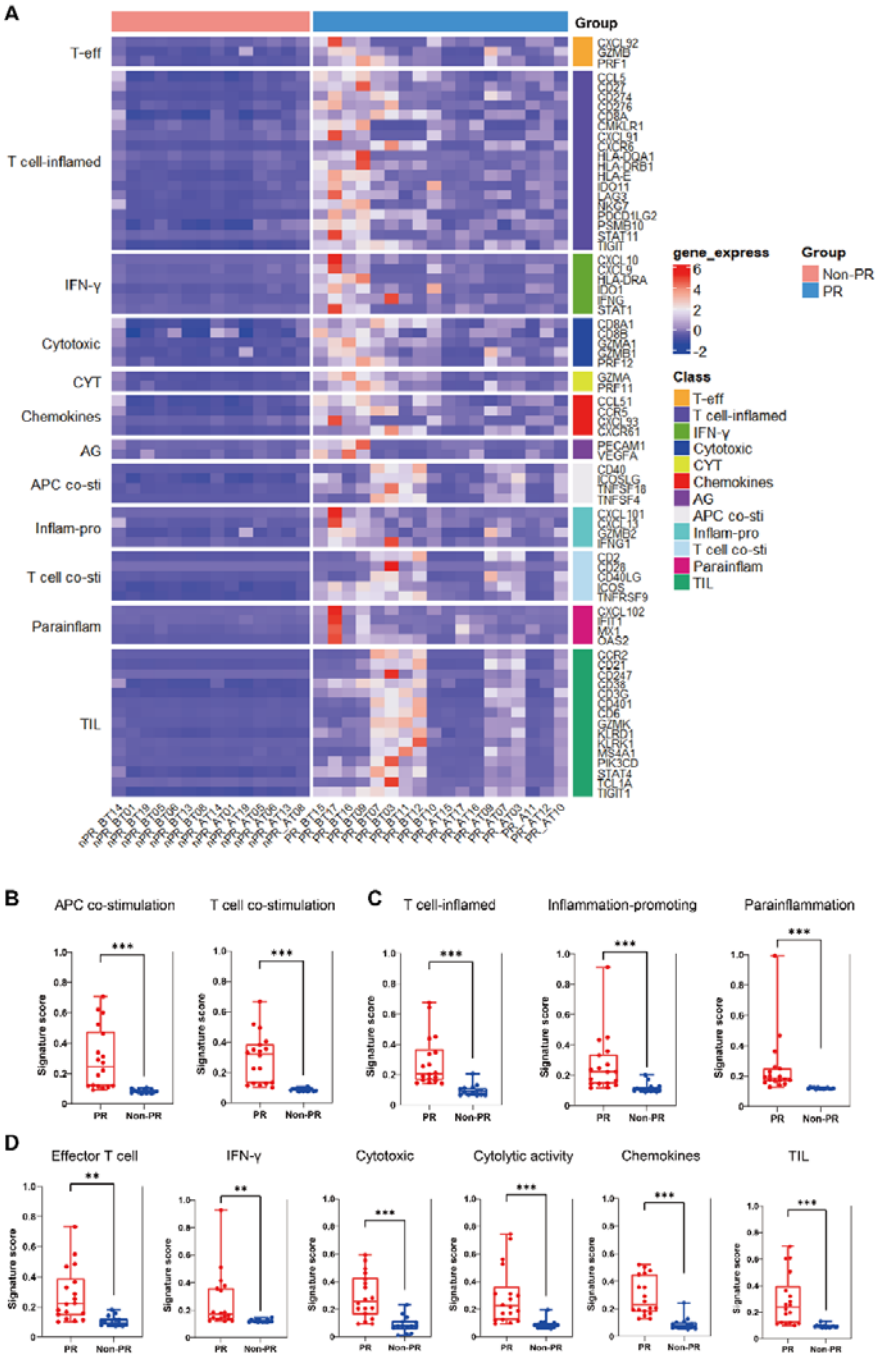

Figure 4. Additional immune signatures analysis. A) The expression of 12 gene sets previously reported to be associated with response to immunotherapy and prognosis between responders (PR) (n = 18) and non-responders (Non-PR) (n = 14). **BCD)** 11 gene sets of prognostic value were differentially expressed between responders (PR) (n = 18) and non-responders (Non-PR) (n = 14), box plots are indicated in terms of minima, maxima, centre, bounds of box and whiskers (interquartile range value), and percentile in the style of Tukey, Wilcoxon test was used to determine the statistical significance between subgroups.

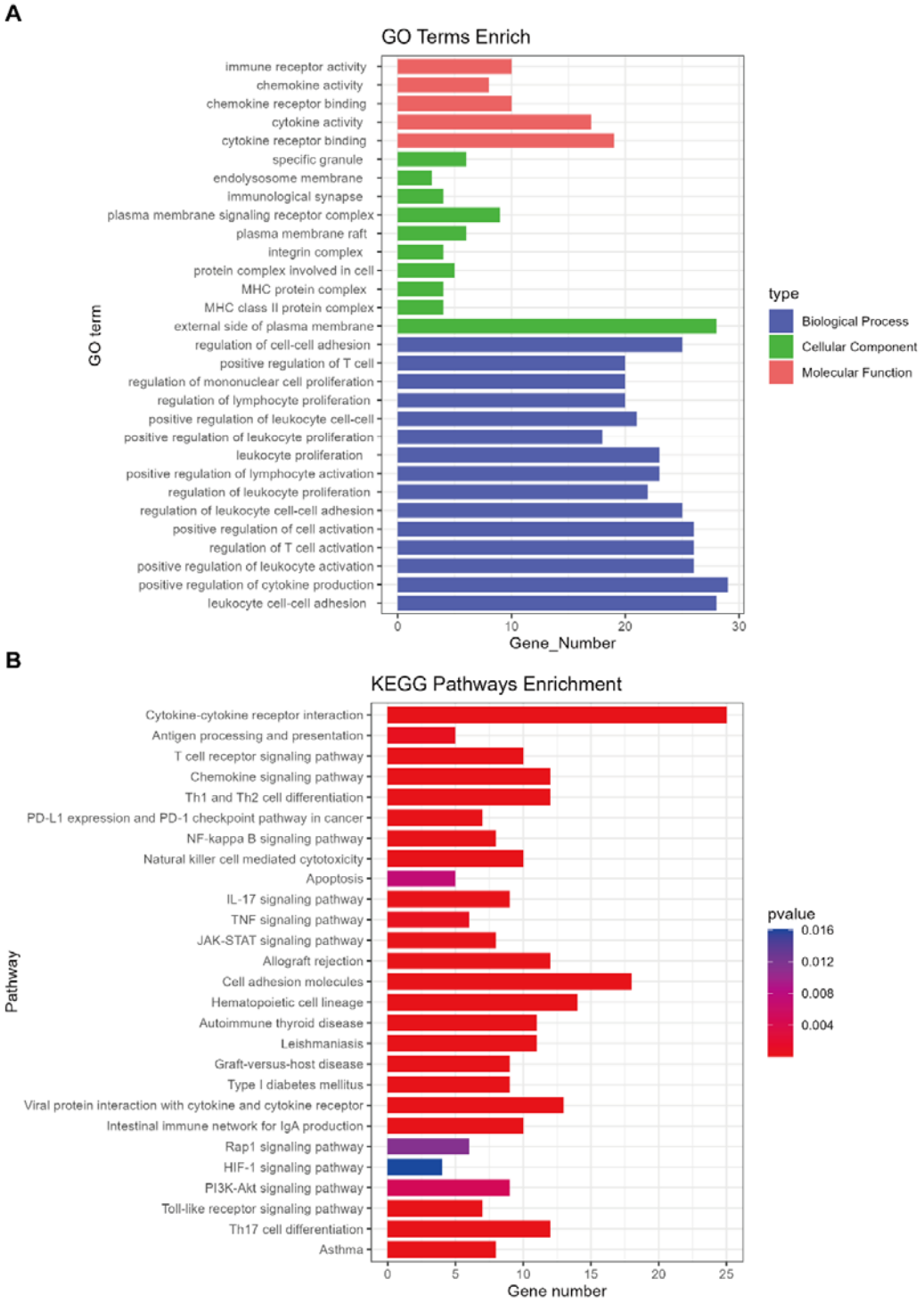

Figure 4-figure supplementary1. GO enrichment and KEGG pathways analysis of differential expression genes. A) GO enrichment analysis were performed to identify the biological process, cellular component and molecular function of differential expression genes. **B)** H KEGG enrichment analysis of differential expression genes.

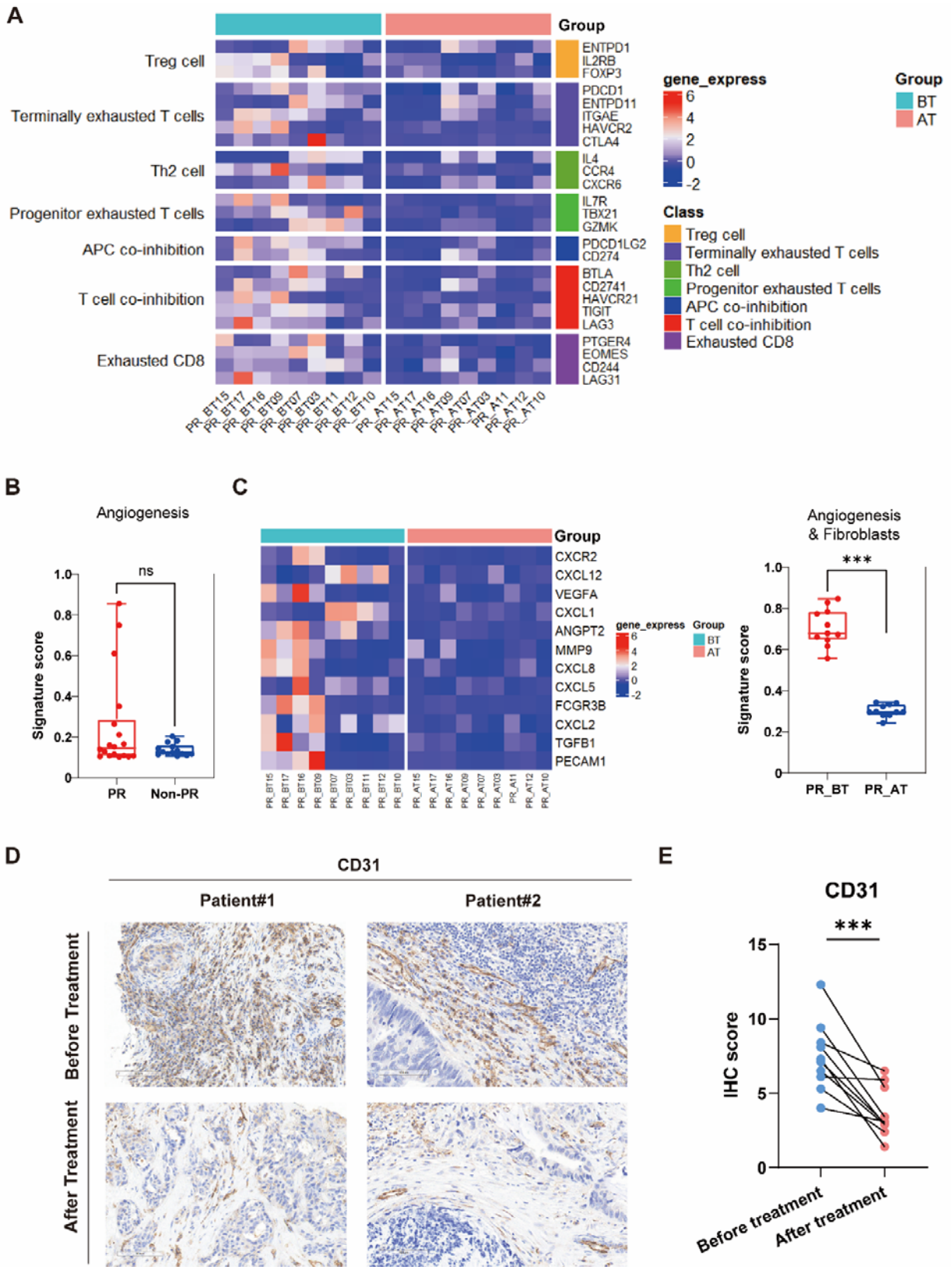
A
Group
Treg cell
Terminally exhausted T cells
Th2 cell
Progenitor exhausted T cells
APC co-inhibition
T cell co-inhibition
Exhausted CD8
ENTPD1
IL2RB
FOXP3
PDCD1
ENTPD11
ITGAE
HAVCR2
CTLA4
IL4
CCR4
CXCR6
IL7R
TBX21
GZMK
PDCD1LG2
CD274
BTLA
CD2741
HAVCR21
TIGIT
LAG3
PTGER4
EOMES
CD244
LAG31
gene_express
6
4
2
0
-2
Group
BT
AT
Class
Treg cell
Terminally exhausted T cells
Th2 cell
Progenitor exhausted T cells
APC co-inhibition
T cell co-inhibition
Exhausted CD8
B
Angiogenesis
ns
Signature score
PR
Non-PR
C
Group
CXCR2
CXCL12
VEGFA
CXCL1
ANGPT2
MMP9
CXCL8
CXCL5
FCGR3B
CXCL2
TGFB1
PECAM1
Angiogenesis
& Fibroblasts
***
PR_BT
PR_AT
D
CD31
Patient#1
Patient#2
Before Treatment
After Treatment
E
CD31
***
IHC score
Before treatment
After treatment

590

591

Figure 5. Comparison of responders before and after treatment A) The expression of 7 gene sets previously reported to be associated with response to immunosuppressive between before treatment (n = 9) and after treatment (n = 9) in the responders (PR). **B)** The expression of Angiogenesis sets between responders (PR) (n = 18) and non-responders (Non-PR) (n = 14). **C)** The expression of Angiogenesis & Fibroblasts sets between before treatment (n = 9) and after treatment (n = 9) in the responders. Box plots are indicated in terms of minima, maxima, centre, bounds of box and whiskers (interquartile range value), and percentile in the style of Tukey, Wilcoxon test was used to determine the statistical significance between subgroups. **D&E)** Representative CD31 IHC staining of before and after treatment specimens of patien

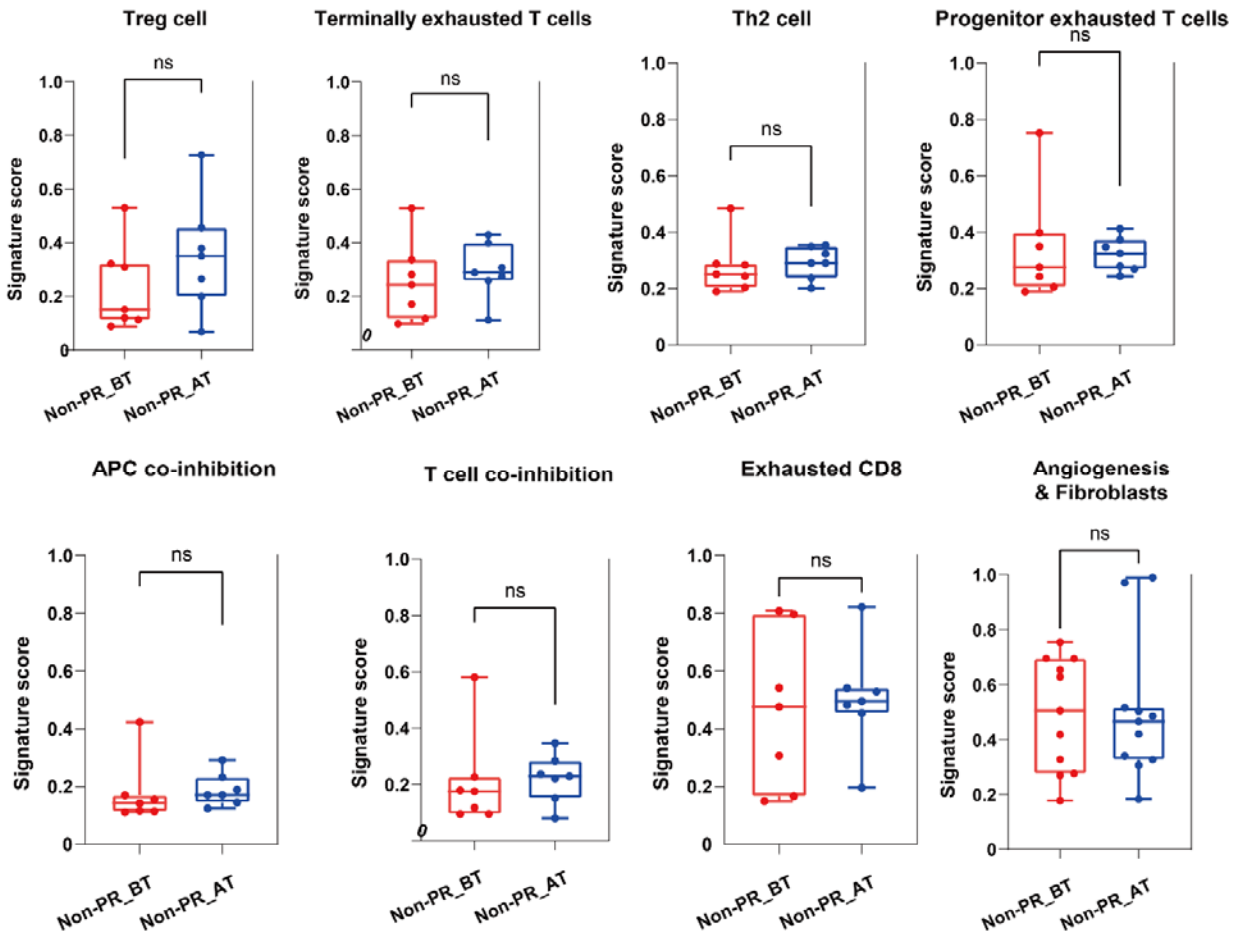

Figure 5-figure supplementary1. Comparison of non-responders before and after treatment.

Appendix

Participants

Inclusion criteria included the presence of at least one measurable lesion assessed according to the Response Evaluation Criteria in Solid Tumors (RECIST) version 1.1 and an Eastern Cooperative Oncology Group (ECOG) performance status of 0 or 1. Patients must have received first-line treatment with fluorouracil, irinotecan, and oxaliplatin (any combination) or have been intolerant to first-line drugs. KPS≥60，PS≤2. Patients were also required to have an expected survival of ≥3 months and adequate organ and bone marrow function (absolute neutrophil count >1000/L, hemoglobin >75 g/L, neutrophils ≥ 1000/μl， blood cells ≥ 75,000/μl，platelet count >100×109/L, prothrombin time <1.5 upper limit of normal (ULN), activated partial thromboplastin time <1.5 ULN, bilirubin ≤1.5×ULN (could be extended to 3×ULN in case of liver metastasis), blood aspartate aminotransferase and alanine aminotransferase ≤3×ULN (could be extended to 5×ULN in case of liver metastasis), serum creatinine level ≤1.58×ULN or creatinine clearance ≥40 mL/min, urinary protein / creatinine ratio < 1 (or urine analysis < 1 + or 24-hour urinary protein < 1g / 24 h). Patients were excluded in the following cases: received previous treatment with any radiation therapy;, received treatment with corticosteroids or other immunosuppressive agents within 14 days prior to study drug administration, presence of autoimmune disease, known interstitial lung disease, and those with previous or concurrent malignancies expect for basal cell carcinoma, cutaneous squamous cell carcinoma, or cervical carcinoma in situ that have undergone radical treatment.

A list of 289 genes of Nanostring panel RNA sequencing.

SDHA	ITGAL	TNFSF13B	CTSW	PTGER4	GNLY
C1QB	PSMB10	HSD11B1	IRF1	CXCR2	PDCD1LG2
BTLA	C1QA	GZMA	TDO2	HERC6	ABCF1
TGFB1	LYZ	ITGA1	CD28	IL17A	IL6
GUSB	CD274	CXCR3	AXL	IL15	FPR1
TNFSF9	IL4	PDCD1	IFI35	CD3D	CD74
ICOS	KIR2DL3	SELL	IL10RA	CD1C	G6PD
PECAM1	IL7R	BRCA1	CCR5	EOMES	EGFR
SPIB	IL21R	CD40	TFRC	TLR7	HLA-DMB
IFIH1	IL2RG	IFIT2	ENTPD1	LY9	HLA-DPA1
MTOR	FCGR2B	HLA-DQA2	ITGAE	HAVCR2	IRF4
TRAT1	CD70	NOS2	LCK	IFNG	CDKN2A
DLL4	CD3E	CD79A	CCR2	FCRL2	EIF2AK2
NFKBIA	RB1	CD68	KIR3DL2	MS4A2	CTAG1B
ADM	HLA-DMA	GZMB	CCL20	CSF3R	MS4A1
HLA-DOB	S100A9	CCL18	MAGEA12	CXCL12	NT5E
CXCL11	CYBB	CD86	TNF	IFIT1	PTPRC
CCR4	CPA3	FGF13	FUT4	ICOSLG	IL2
CD40LG	CD209	CCL22	IFI27	VEGFA	BRCA2
CD163	NKG7	CCL2	STAT4	TLR9	IL12RB2

PRF1	CD44	IL2RB	ITGAM	CXCL9	TBP
CD244	CXCR4	PTEN	TNFRSF9	MRC1	CXCL1
GZMH	SNAI1	MS4A4A	TCL1A	TNFSF18	IDO1
CD247	VTCN1	MKI67	CCL21	TIGIT	ATM
CD48	PSMB9	LILRB2	CSF2	PDGFB	IL18
IL10	TNFSF10	SIGLEC5	VCAM1	HDC	MAGEA4
ANGPT2	PMS2	TAP1	RAD51	CD276	S100A8
CD80	CCL13	BIRC5	CD3G	ZAP70	ISG15
ZEB1	CTSS	TNFRSF14	TNFRSF18	PVR	MMP9
CD69	PIK3CA	TNFRSF4	PTGS2	BLK	IL1A
CEACAM3	CMKLR1	ARG1	S100A12	OAS3	TWIST1
CD84	PNOC	TNFRSF17	IL1B	BLM	CCL5
KLRD1	CD8A	PIK3CD	RUNX3	CSF1R	ADORA2A
IFIT3	CCL4	HLA-DOA	CX3CR1	IFI6	BRIP1
CD47	CCND1	TNFRSF1B	IRF9	SH2D1A	MAGEA1
CXCL8	IFITM2	CD38	CD27	NECTIN2	MLANA
ITGB2	TLR3	CXCL5	STAT3	AKT1	ITGAX
CTLA4	MAGEC2	PDGFA	FCGR1A	MLH1	KLRK1
TBX21	TNFRSF1A	FOXP3	MYC	TIE1	SLAMF7
MELK	GBP1	CD8B	CD79B	CD14	CXCL13
MX1	TNFSF4	CSF2RB	RORC	FCAR	CCL7
KLRB1	PTPN11	BCL2	CD2	HLA-DRA	LAG3
MSH2	KIR3DL1	TLR8	CD4	CXCL10	ICAM1
CX3CL1	FASLG	OAS2	CXCR6	HIF1A	NCAM1
GZMK	POLR2A	NCR1	NBN	OAS1	IFITM1
CD19	FAS	CD6	STAT1	MSH6	IL2RA
TPSAB1	HLA-DQA1	PRR5	GZMM	HLA-E	PF4
HLA-DRB1	UBB	OAZ1	TBC1D10B	FCGR3B	CXCL2
STK11IP					

A

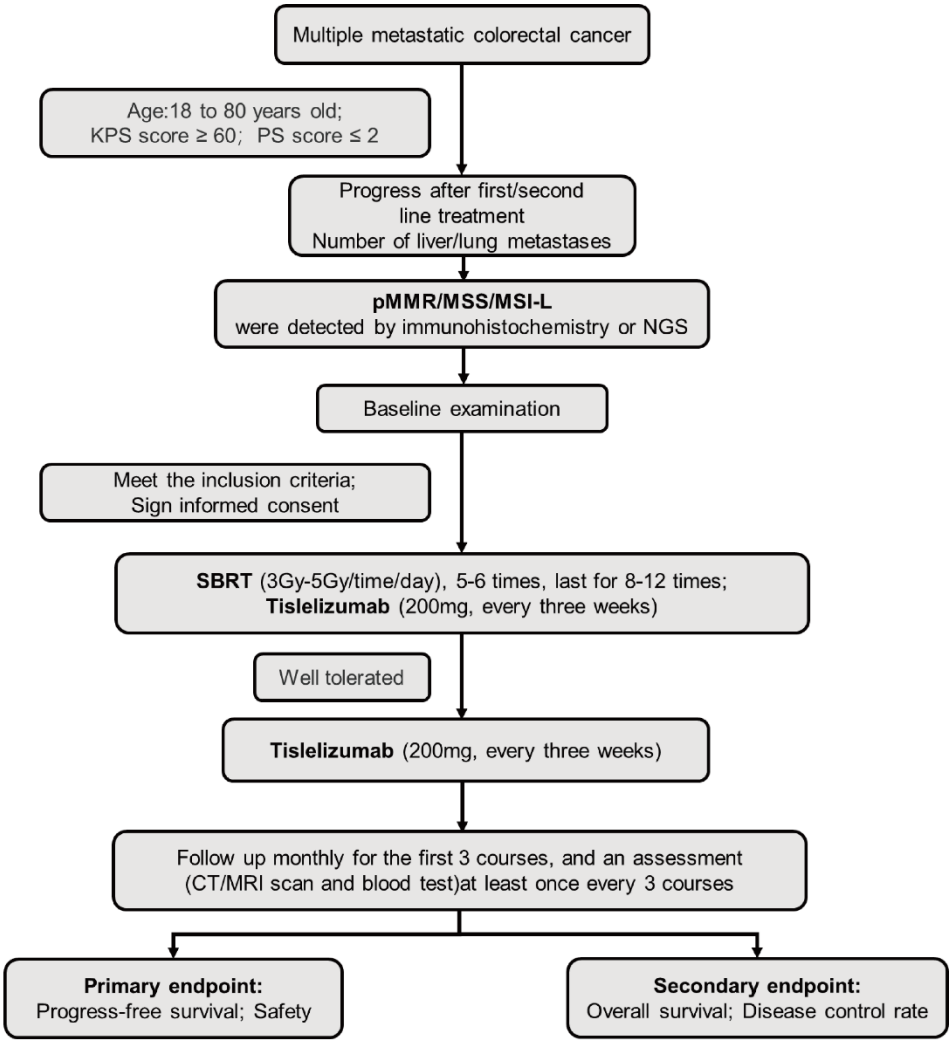
Multiple metastatic colorectal cancer
Age:18 to 80 years old;
KPS score ≥ 60; PS score ≤ 2
Progress after first/second line treatment
Number of liver/lung metastases
pMMR/MSS/MSI-L
were detected by immunohistochemistry or NGS
Baseline examination
Meet the inclusion criteria;
Sign informed consent
SBRT (3Gy-5Gy/time/day), 5-6 times, last for 8-12 times;
Tislelizumab (200mg, every three weeks)
Well tolerated
Tislelizumab (200mg, every three weeks)
Follow up monthly for the first 3 courses, and an assessment
(CT/MRI scan and blood test)at least once every 3 courses
Primary endpoint:
Progress-free survival; Safety
Secondary endpoint:
Overall survival; Disease control rate

B

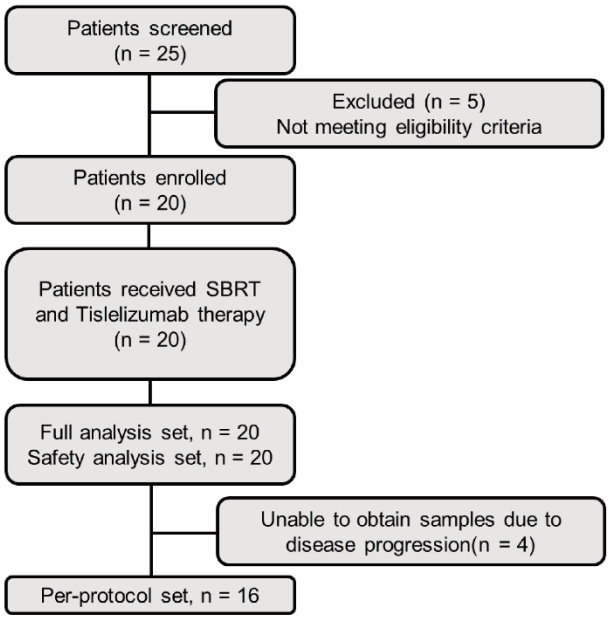
Patients screened
(n = 25)
Excluded (n = 5)
Not meeting eligibility criteria
Patients enrolled
(n = 20)
Patients received SBRT
and Tislelizumab therapy
(n = 20)
Full analysis set, n = 20
Safety analysis set, n = 20
Unable to obtain samples due to
disease progression(n = 4)
Per-protocol set, n = 16

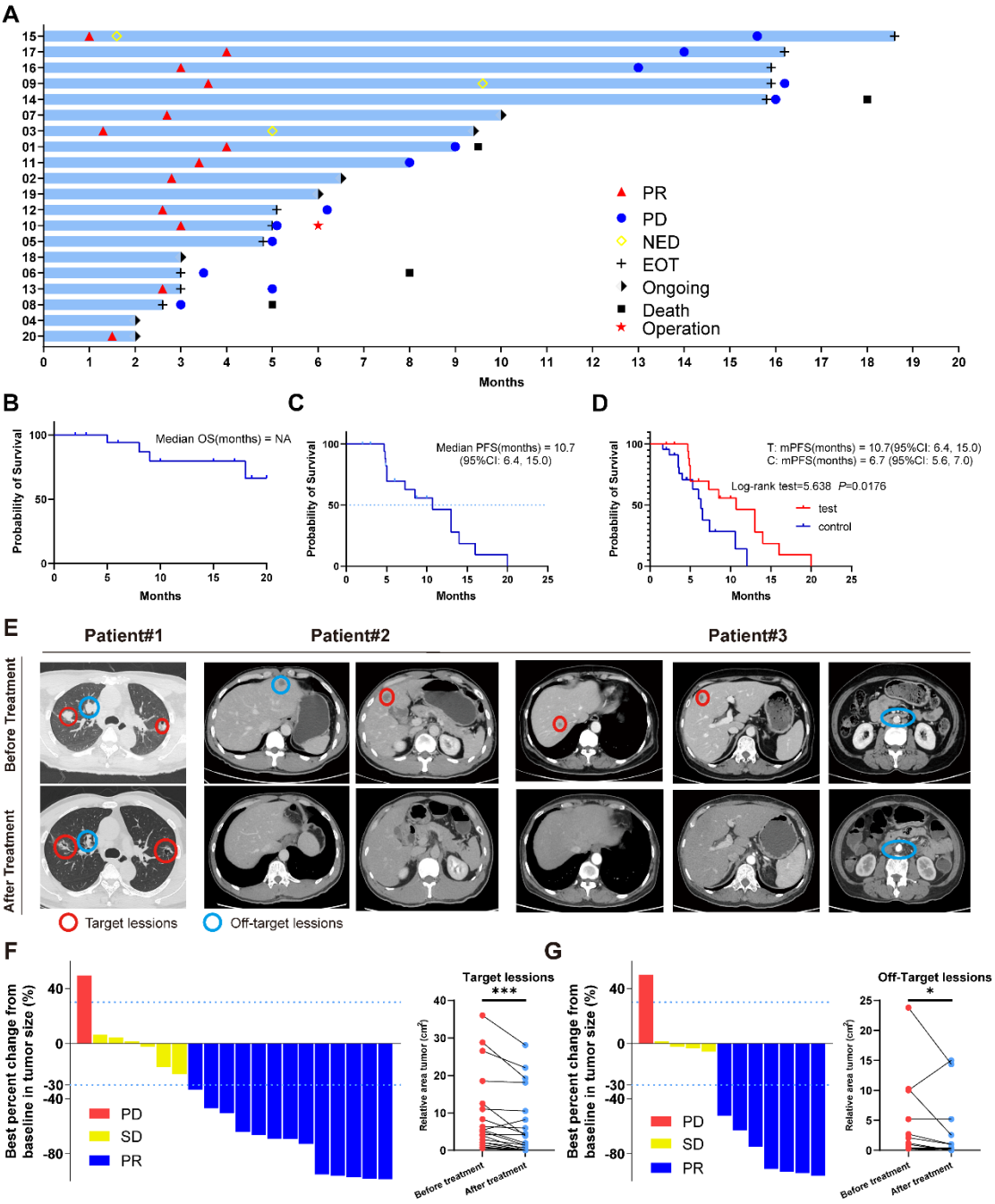
A
15
17
16
09
14
07
03
01
11
02
19
12
10
05
18
06
13
08
04
20
PR
PD
NED
EOT
Ongoing
Death
Operation
Months
B
Median OS(months) = NA
Probability of Survival
Months
C
Median PFS(months) = 10.7
(95%CI: 6.4, 15.0)
Probability of Survival
Months
D
T: mPFS(months) = 10.7(95%CI: 6.4, 15.0)
C: mPFS(months) = 6.7 (95%CI: 5.6, 7.0)
Log-rank test=5.638 P=0.0176
test
control
Probability of Survival
Months
E
Patient#1
Patient#2
Patient#3
Before Treatment
After Treatment
Target lessions
Off-target lessions
F
Best percent change from baseline in tumor size (%)
PD
SD
PR
Target lessions
***
Relative area tumor (cm²)
Before treatment
After treatment
G
Best percent change from baseline in tumor size (%)
PD
SD
PR
Off-Target lessions
*
Relative area tumor (cm²)
Before treatment
After treatment

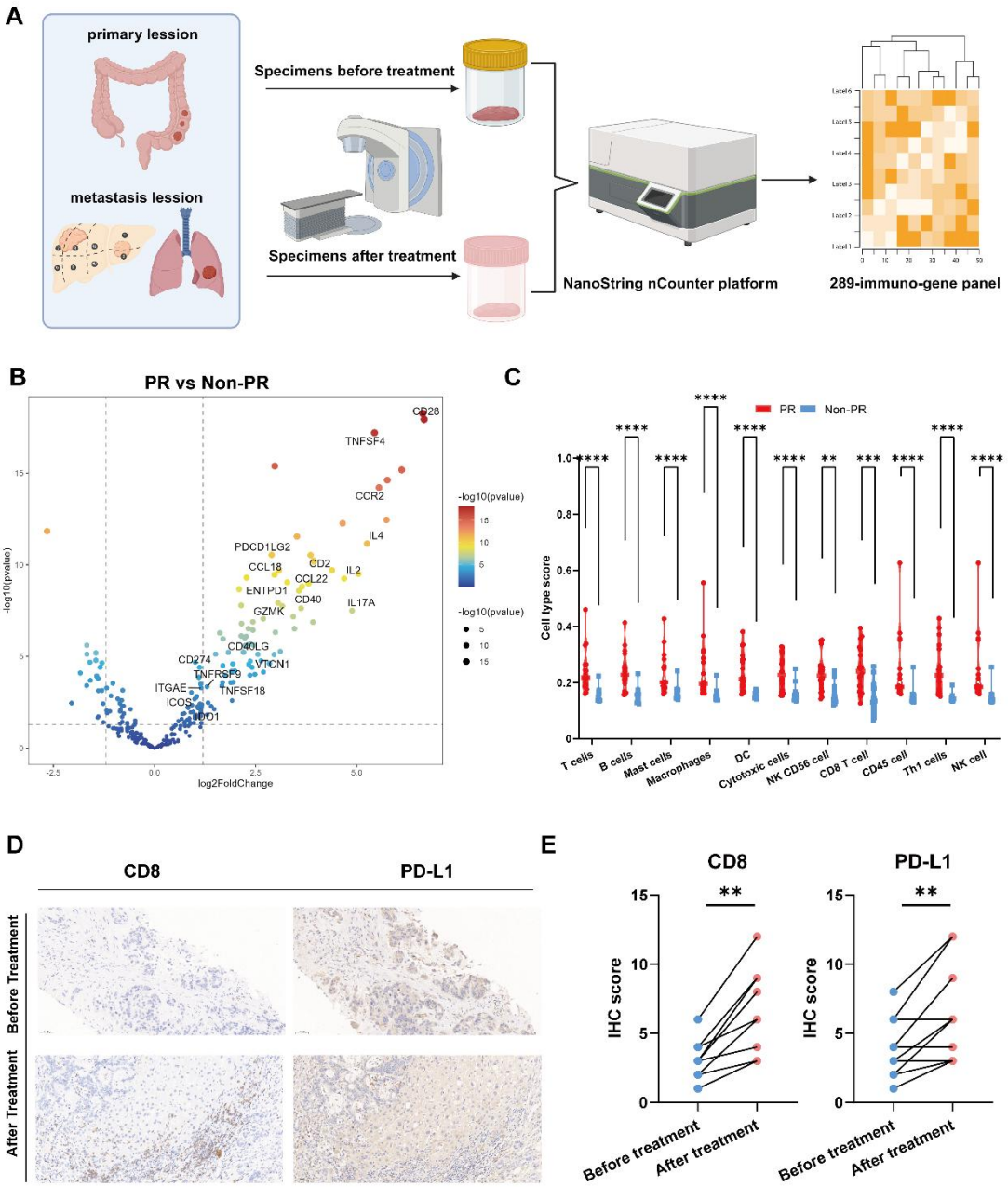
A
primary lession
metastasis lession
Specimens before treatment
Specimens after treatment
NanoString nCounter platform
289-immuno-gene panel
B
PR vs Non-PR
-log10(pvalue)
log2FoldChange
CD28
TNFSF4
CCR2
IL4
PDCD1LG2
CCL18
CD2
IL2
CCL22
ENTPD1
CD40
IL17A
GZMK
CD40LG
CD274
VTCN1
TNFRSF9
ITGAE
TNFSF18
ICOS
IDO1
C
PR
Non-PR
Cell type score
T cells
B cells
Mast cells
Macrophages
DC
Cytotoxic cells
NK CD56 cell
CD8 T cell
CD45 cell
Th1 cells
NK cell
D
CD8
PD-L1
Before Treatment
After Treatment
E
CD8
PD-L1
IHC score
Before treatment
After treatment

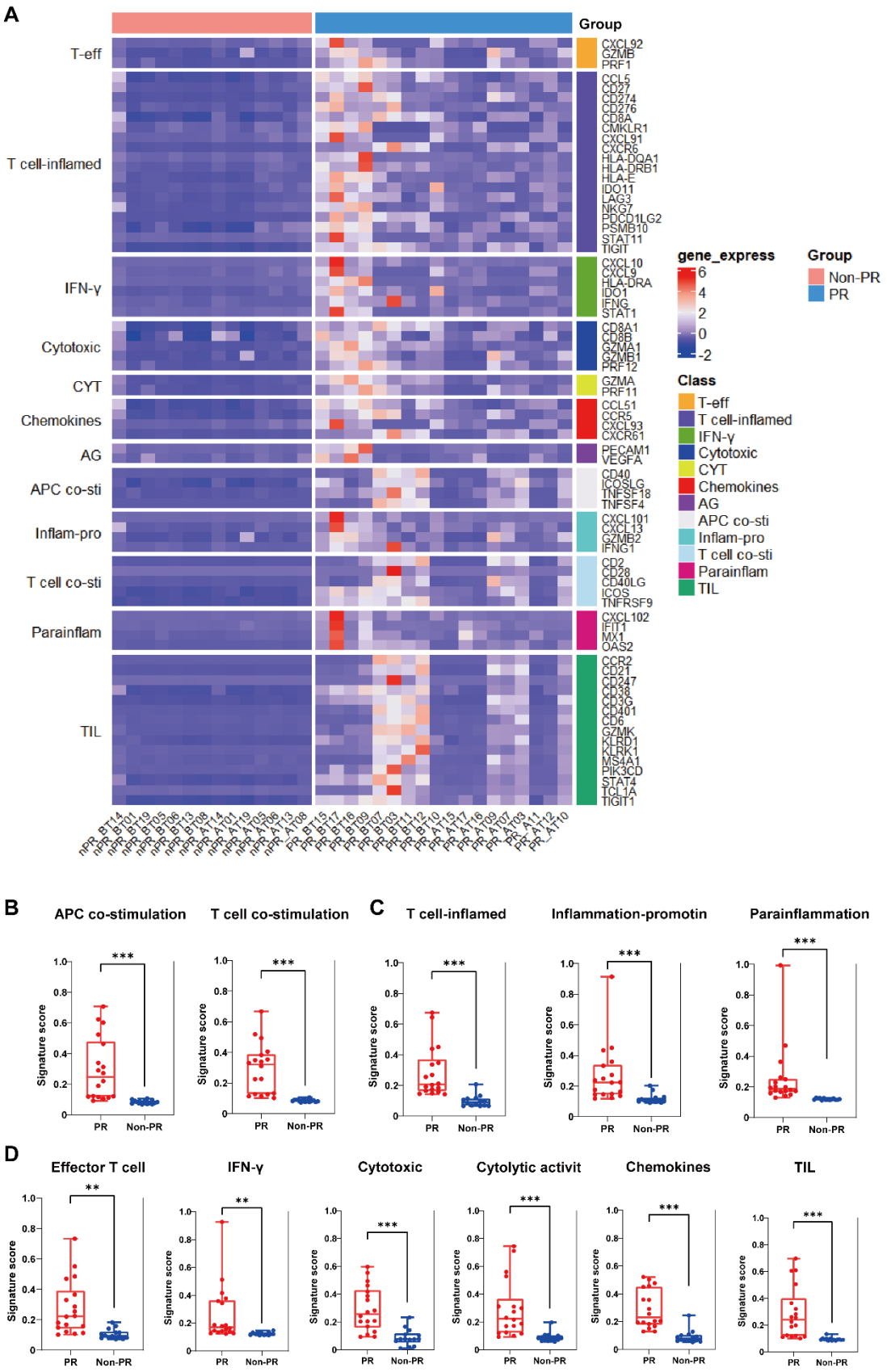
A
Group
T-eff
CXCL92
GZMB
PRF1
T cell-inflamed
CCL5
CD27
CD274
CD276
CD8A
CMKLR1
CXCL91
CXCR6
HLA-DQA1
HLA-DRB1
HLA-E
IDO11
LAG3
NKG7
PDCD1LG2
PSMB10
STAT11
TIGIT
IFN-γ
CXCL10
CXCL9
HLA-DRA
IDO1
IFNG
STAT1
Cytotoxic
CD8A1
CD8B
GZMA1
GZMB1
PRF12
CYT
GZMA
PRF11
Chemokines
CCL51
CCR5
CXCL93
CXCR61
AG
PECAM1
VEGFA
APC co-sti
CD40
ICOSLG
TNFSF18
TNFSF4
Inflam-pro
CXCL101
CXCL13
GZMB2
IFNG1
T cell co-sti
CD2
CD28
CD40LG
ICOS
TNFRSF9
Parainflam
CXCL102
IFIT1
MX1
OAS2
TIL
CCR2
CD21
CD247
CD38
CD3G
CD401
CD6
GZMK
KLRD1
KLRK1
MS4A1
PIK3CD
STAT4
TCL1A
TIGIT1
gene_express
6
4
2
0
-2
Group
Non-PR
PR
Class
T-eff
T cell-inflamed
IFN-γ
Cytotoxic
CYT
Chemokines
AG
APC co-sti
Inflam-pro
T cell co-sti
Parainflam
TIL
B
APC co-stimulation
T cell co-stimulation
C
T cell-inflamed
Inflammation-promotin
Parainflammation
D
Effector T cell
IFN-γ
Cytotoxic
Cytolytic activit
Chemokines
TIL
Signature score
PR
Non-PR
***
**

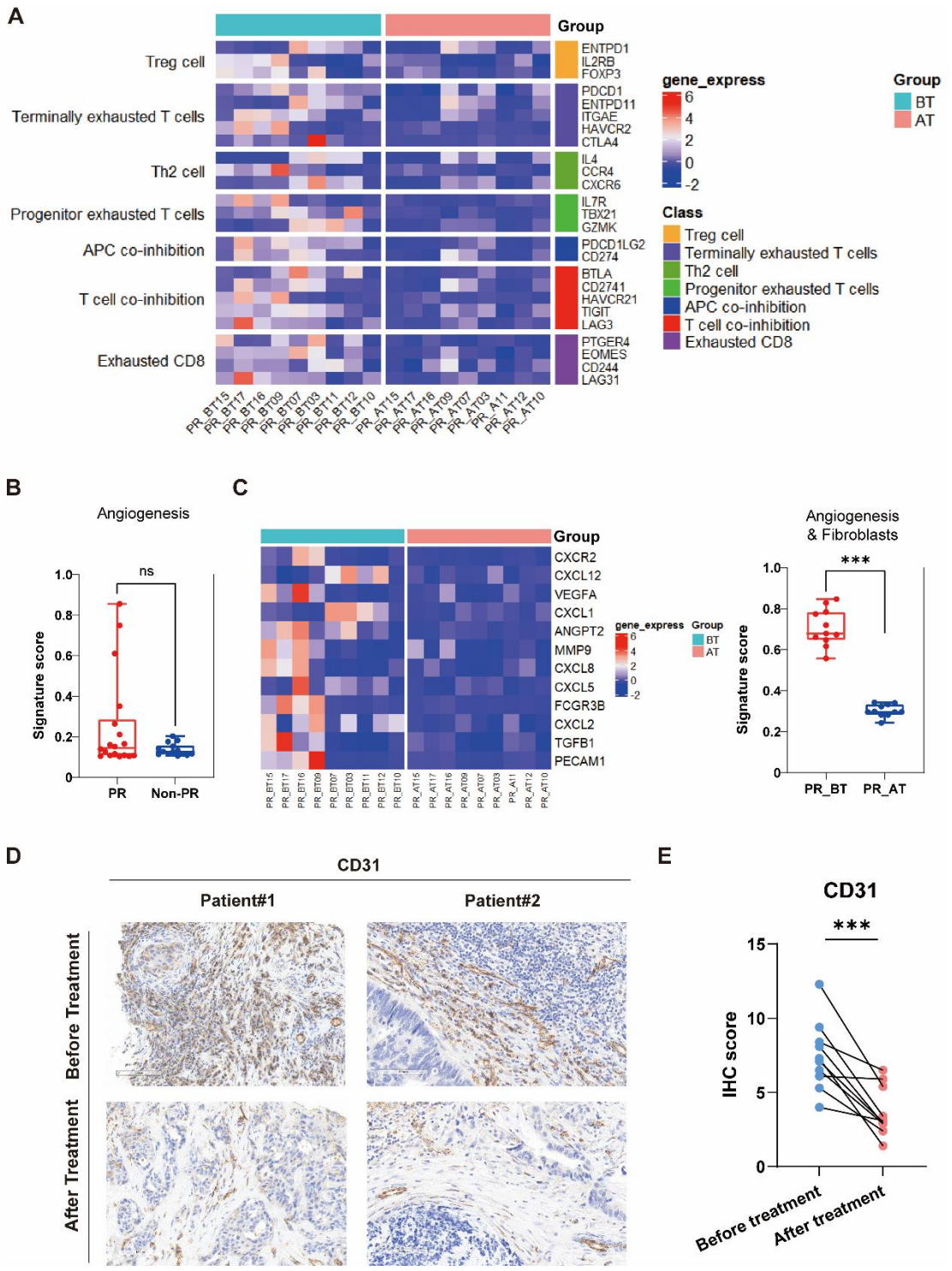
A
Group
Treg cell
Terminally exhausted T cells
Th2 cell
Progenitor exhausted T cells
APC co-inhibition
T cell co-inhibition
Exhausted CD8
ENTPD1
IL2RB
FOXP3
PDCD1
ENTPD11
ITGAE
HAVCR2
CTLA4
IL4
CCR4
CXCR6
IL7R
TBX21
GZMK
PDCD1LG2
CD274
BTLA
CD2741
HAVCR21
TIGIT
LAG3
PTGER4
EOMES
CD244
LAG31
gene_express
6
4
2
0
-2
Group
BT
AT
Class
Treg cell
Terminally exhausted T cells
Th2 cell
Progenitor exhausted T cells
APC co-inhibition
T cell co-inhibition
Exhausted CD8
B
Angiogenesis
ns
Signature score
PR
Non-PR
C
Group
CXCR2
CXCL12
VEGFA
CXCL1
ANGPT2
MMP9
CXCL8
CXCL5
FCGR3B
CXCL2
TGFB1
PECAM1
Angiogenesis
& Fibroblasts
***
Signature score
PR_BT
PR_AT
D
CD31
Patient#1
Patient#2
Before Treatment
After Treatment
E
CD31
***
IHC score
Before treatment
After treatment